



Smart design of Rh-based hydrogen evolution electrocatalysts: integrating DFT, machine learning, and structural optimization for sustainable hydrogen energy

Jitang Zhang¹, Lei Tian¹, Shijie Shen^{1,2}, Huanhuan Zhang¹, Lianli Jia³, Xinxing Shi^{1,3}, Wenwu Zhong², Lili Zhang^{1,*}, Chenglong Qiu^{1,*}, Jiacheng Wang^{1,*}

Keywords:

Rh-based electrocatalysts, water splitting, hydrogen evolution reaction, theoretical calculation, machine learning

Citation:

Zhang, J.; Tian, L.; Shen, S.; Zhang, H.; Jia, L.; Shi, X.; Zhong, W.; Zhang, L.; Qiu, C.; Wang, J. Smart design of Rh-based hydrogen evolution electrocatalysts: integrating DFT, machine learning, and structural optimization for sustainable hydrogen energy. *Energy Mater.* 2026, 6, 600010.

<https://dx.doi.org/10.20517/energymater.2025.148>

Received: 10 Sep 2025

First Decision: 11 Oct 2025

Revised: 31 Oct 2025

Accepted: 25 Nov 2025

Published: 26 Jan 2026

Academic Editor:

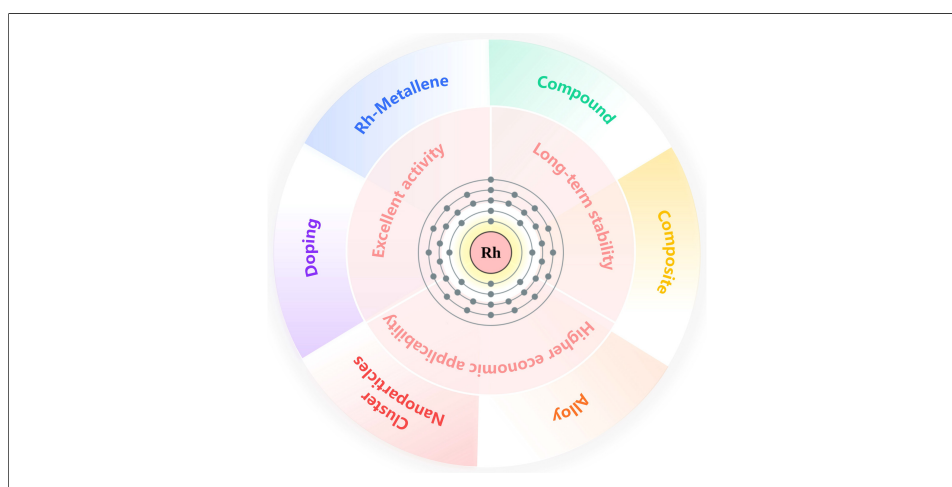
Yuhui Chen

Copy Editor:

Fangling Lan

Production Editor:

Fangling Lan



Abstract

Hydrogen energy is vital for achieving carbon neutrality, with green hydrogen from water electrolysis being key. The hydrogen evolution reaction (HER) critically determines system viability, driving the search for high-performance, stable and affordable electrocatalysts. Rhodium (Rh)-based catalysts are promising platinum alternatives due to near-ideal hydrogen adsorption energy, tunable electronic structure, and stable activity across all pH ranges. This review highlights recent advances in Rh-based HER catalysts, including mechanisms, descriptors, materials, and optimization strategies. Density functional theory (DFT) indicates that Rh catalysts typically follow the Volmer-Heyrovsky-Tafel pathway, with performance governed by surface geometry and electronic states. Key activity descriptors are summarized, while combining DFT with machine learning enables high-throughput screening and rational catalyst design. Experimentally, activity and stability are improved through atomic-scale modulation, interface engineering, and carrier synergy. Rh-based catalysts are categorized into single atoms, nanoclusters, 2D metallenes, nanoparticles, and compounds (phosphides, sulfides, oxides, nitrides), with

¹Zhejiang Key Laboratory for Island Green Energy and New Materials, School of Materials Science and Engineering, Taizhou University, Taizhou 318000, Zhejiang, China.

²Zhejiang Key Laboratory of Functional Ionic Membrane Materials and Technology for Hydrogen Production, Shaoxing University, Shaoxing 312000, Zhejiang, China.

³College of Materials Science and Engineering, Jiamusi University, Jiamusi 154007, Heilongjiang, China.

*Correspondence to: Dr. Lili Zhang, Zhejiang Key Laboratory for Island Green Energy and New Materials, School of Materials Science and Engineering, Taizhou University, Taizhou 318000, Zhejiang, China. E-mail: zhanglily@tzc.edu.cn; Dr. Chenglong Qiu, Zhejiang Key

Laboratory for Island Green Energy and New Materials, School of Materials Science and Engineering, Taizhou University, Taizhou 318000, Zhejiang, China. E-mail: qiuchenglong@tzc.edu.cn; Dr. Jiacheng Wang, Zhejiang Key Laboratory for Island Green Energy and New Materials, School of Materials Science and Engineering, Taizhou University, Taizhou 318000, Zhejiang, China. E-mail: jiacheng.wang@tzc.edu.cn

synthesis methods and performance characteristics reviewed. Remaining challenges include reducing synthesis cost, ensuring long-term durability, and achieving scalable production. Future research should deepen structure-activity understanding and integrate artificial intelligence to accelerate the development of practical Rh-based HER catalysts.

INTRODUCTION

Under the pressing global energy transition, hydrogen energy - as a clean, efficient, and sustainable energy carrier - is increasingly becoming a research hotspot and a pivotal player in future energy landscapes^[1-4]. Water electrolysis, with its notable advantages of relatively simple processes and high product purity, is regarded as one of the most promising pathways for large-scale hydrogen production^[5-10]. In water electrolysis, the hydrogen evolution reaction (HER) as the core step, directly determines hydrogen production energy consumption and costs, making the development of high-performance HER catalysts critical^[3,11-14]. Rhodium (Rh)-based materials have emerged as a focal point among various HER catalysts due to their unique electronic structures and exceptional catalytic properties^[15]. There are some unique advantages and distinctions of Rh compared with other noble metals, such as platinum (Pt), Iridium (Ir), Ruthenium (Ru), and Palladium (Pd), when used as HER electrocatalysts. First, hydrogen binding energy: Rh exhibits an optimal hydrogen adsorption free energy ($\Delta G_{\text{H}^*} \approx 0$ eV), comparable to that of Pt but with greater electronic tunability, which enables high intrinsic HER activity in both acidic and alkaline media^[6,16]. Second, pH universality: Unlike Ir or Ru, which often perform well only in specific pH conditions^[17], Rh-based catalysts maintain excellent stability and activity across a wide pH range. Third, anti-poisoning and durability: Rh demonstrates stronger tolerance toward surface poisoning (e.g., CO or S species) and superior corrosion resistance compared to Pt and Pd, contributing to long-term operational stability. Finally, cost-performance balance: although Rh is a noble metal, its mass-specific activity is higher and atom utilization efficiency is superior to that of Pt, allowing cost reduction through alloying or single-atom dispersion strategies^[18], offering potential for cost reduction in large-scale applications^[19-21]. Moreover, while significant progress has been made in developing non-precious metal catalysts (NPMCs) such as transition metal phosphides, sulfides, and carbides for the HER^[22-24], these systems often face a compromise between activity, stability, and operational versatility. For instance, MoS₂ exhibits notable activity primarily in acidic media^[25], while many Ni-based catalysts are optimal in alkaline conditions, with their long-term durability under high current densities remaining a concern^[26]. In this context, Rh emerges as a compelling alternative, presenting a unique set of catalytic properties that bridge the gap between ultra-high performance and robust stability. Theoretical and experimental studies confirm that Rh possesses a ΔG_{H^*} nearly as optimal as Pt, endowing it with superior intrinsic activity. Crucially, Rh surpasses Pt in its inherent corrosion resistance and electrochemical stability, particularly in harsh acidic environments or under oxidative potentials, suggesting potentially superior longevity^[18]. When compared to NPMCs, the distinction of Rh lies in its exceptional all-rounder capability. It not only rivals the best NPMCs in intrinsic activity but, more importantly, maintains this high performance across the entire pH spectrum while exhibiting exceptional structural and chemical integrity that most earth-abundant alternatives cannot match^[27].

Early studies focused on exploring the intrinsic HER activity of metallic Rh, revealing its ΔG_{H^*} close to that of Pt in acidic media, demonstrating favorable electrocatalytic performance. To reduce noble metal costs, researchers subsequently attempted to form alloys of Rh with non-noble metals such as Ni and Co (e.g., Rh-Ni, Rh-Co)^[28-31], aiming to achieve synergistic catalytic effects through electronic modulation and

geometric structure optimization. Entering the 21st century, advancements in nanotechnology spurred investigations into Rh-based nanostructures such as nanoparticles^[32–35] and nanosheets^[36]. Research emphasis shifted toward enhancing catalytic activity and atomic utilization by exposing high-index facets, tuning particle sizes, and engineering morphologies. Representative achievements during this phase included ultrafine Rh nanoparticles, polyhedral facet engineering, and carbon-supported Rh nanocomposites^[34,37–39]. With the rise of single-atom catalysis (SAC) and cluster catalysis, Rh-based materials have entered a new era of atomic-level precision. Single-atom Rh catalysts, leveraging their maximal atomic utilization and unique coordination environments, have emerged as a research hotspot for achieving exceptional HER performance at ultralow loadings^[18,40]. Concurrently, low-coordination Rh cluster catalysts have drawn attention due to their abundant active sites and distinctive electronic configurations^[6,41]. To further enhance catalytic performance and stability, research has gradually shifted toward composite systems integrating Rh with functional materials such as MoS₂, TiO₂, and nitrogen (N)-doped carbon^[27,42]. By harnessing carrier synergies, electronic structure modulation, and interface engineering, hierarchical porous architectures with strong interfacial coupling and high stability are being constructed. With the aid of density functional theory (DFT) calculations and machine learning algorithms, the design of Rh-based HER catalysts is progressively transitioning into an intelligent “computational-driven experimental validation” phase. Researchers utilize descriptors such as ΔG_{H^+} , d-band center, and charge transfer quantities for activity prediction, while high-throughput screening and structure-performance mapping accelerate the development of efficient, low-cost Rh-based HER materials.

In recent years, driven by rapid advancements in materials science and catalytic technologies, significant progress has been made in Rh-based HER catalyst research. From novel synthesis methods to innovative structural designs, and from mechanistic insights to practical applications, these studies continuously push the performance boundaries of Rh-based HER catalysts^[43]. However, despite these achievements, challenges remain, including further improving catalyst activity and stability, optimizing synthesis processes to reduce costs, and deepening the understanding of structure-activity relationships in complex reaction environments. This review aims to comprehensively outline the current research landscape of Rh-based hydrogen evolution catalysts, systematically summarize recent advances in their structural features, catalytic performance, and reaction mechanisms, critically analyze existing challenges, and propose future research directions to advance the development and large-scale industrial application of Rh-based HER catalysts.

COMPARING HER MECHANISMS FOR TRADITIONAL CATALYSTS AND RH-BASED CATALYSTS

HER mechanisms of traditional catalysts

In different pH environments, HER on Rh-based catalysts follows distinct pathways. DFT calculations not only precisely resolve energy changes and electron transfer processes at each reaction stage but also elucidate the role of active sites, significantly deepening mechanistic understanding.

Acidic media

In acidic media, the HER proceeds via the Volmer, Heyrovsky and Tafel steps [Figure 1]^[44–46], with the overall reaction: The Volmer step under acidic conditions is $H^+ + e^- = H_{ads}$ ^[46], H_{ads} is clarified as the adsorbed hydrogen intermediate on the catalyst surface during the HER. The electronic structure of the catalyst significantly affects the rate of this reaction. For example, in Rh-alloy catalysts, the addition of alloying elements changes the electron-cloud distribution around Rh atoms^[47], thereby influencing the adsorption ability of the active sites. Moreover, the geometric structure of the catalyst surface also affects the Volmer step. Defects such as steps, kinks and vacancies on the catalyst surface have high activity due to the coordination unsaturation of atoms, which can lower the adsorption energy barrier and accelerate this step. The Heyrovsky step is expressed as $H^+ + H_{ads} + e^- = H_2$ ^[46]. In this step, the catalyst surface acquires protons

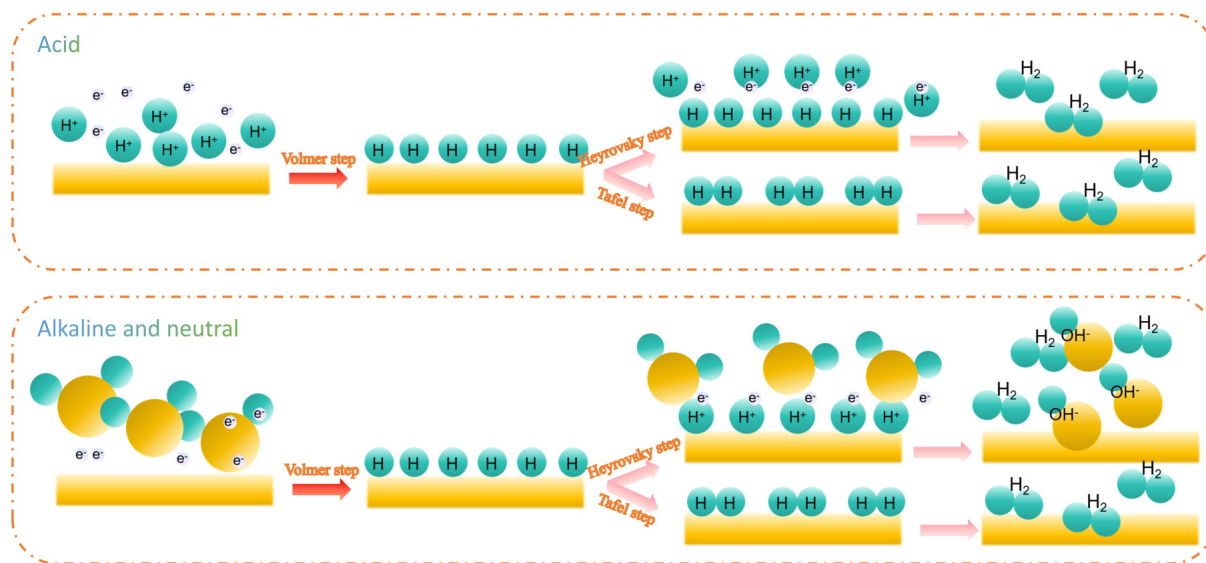


Figure 1. Reaction mechanisms of HER in acid, alkaline, and neutral media.

and electrons, which combine with the adsorbed hydrogen to form hydrogen molecules. DFT simulations show that the reaction energy barrier of this step is closely related to the hydrogen adsorption strength on the catalyst surface. When the hydrogen adsorption is too strong, the formation and desorption of H_2 molecules need to overcome a high energy barrier; when the adsorption is too weak, hydrogen species may desorb from the catalyst surface before participating in the reaction. Both of these extreme situations can inhibit the progress of the HER. Through DFT calculations, Rh-based catalysts with appropriate adsorption strength can be designed to optimize the reaction kinetics of the Heyrovsky step. The Tafel step is $\text{H}_{\text{ads}} + \text{H}_{\text{ads}} = \text{H}_2$; that is, two hydrogen atoms adsorbed on the catalyst surface directly combine to form hydrogen molecules^[46]. DFT calculations show that the reaction energy barrier of the Tafel step is related to the H^+ coverage. When the H^+ coverage is high, the probability of two adsorbed hydrogen atoms meeting and combining increases, which is beneficial for the Tafel step^[22]. However, an excessively high coverage will occupy a large number of active sites, inhibiting the Volmer step and thus reducing the overall reaction rate.

Alkaline media

In alkaline media, the HER pathway also includes the Volmer, Heyrovsky and Tafel steps [Figure 1]. The Volmer step under alkaline conditions is $\text{H}_2\text{O} + \text{e}^- \rightarrow \text{H}_{\text{ads}} + \text{OH}^-$ ^[22,46], which is the rate-controlling step; its reaction energy barrier is higher than that of the Volmer step in acidic media. By introducing metal oxide supports with oxygen vacancies^[47], the adsorption and activation ability of H_2O can be enhanced, and the energy barrier of the Volmer step can be lowered. Oxygen vacancies^[47], as Lewis acid sites, can attract H_2O molecules and promote the breaking of the H-OH bond. The reaction mechanisms of the Heyrovsky and Tafel steps in alkaline media are similar to those in acidic media. However, due to the presence of a large number of OH^- in the alkaline environment, they will compete for the active sites on the catalyst surface, affecting the adsorption and reaction of H^+ . DFT calculations can help understand the influence of OH^- ions and optimize the adsorption and desorption processes of H^+ by designing appropriate catalyst structures to promote the progress of these two steps.

Neutral media

In neutral media, the overall HER is also $2\text{H}_2\text{O} + 2\text{e}^- \rightarrow \text{H}_2 + 2\text{OH}^-$ ^[48,49]. However, due to the lack of a large number of H^+ or OH^- , its reaction mechanism is more complex. Under neutral conditions, the reaction starts

with the adsorption and dissociation of water molecules on the surface of Rh-based catalysts. DFT calculations show that the surface properties of the catalyst have a significant impact on the adsorption mode and adsorption energy of water molecules^[50]. On the surface of Rh nanoparticles with specific crystal planes, water molecules can be adsorbed in a specific orientation, reducing the energy barrier for dissociation. In addition, introducing suitable support or doping atoms can change the electronic structure of the catalyst surface, promoting the adsorption and dissociation of water molecules. The adsorption and reaction of the dissociated hydrogen atoms on the catalyst surface determine the subsequent reaction pathway. Similar to acidic and alkaline media, appropriate adsorption energy is crucial for efficient hydrogen evolution. DFT calculations can predict the adsorption energy of different-structured Rh-based catalysts for hydrogen atoms. By optimizing the catalyst structure, the balance between adsorption and desorption can be achieved, promoting the progress of the HER. Through DFT calculations, the microscopic mechanism of the HER on Rh-based catalysts under different pH conditions can be comprehensively understood, providing a solid theoretical basis for the design of efficient Rh-based hydrogen evolution catalysts.

Hydrogen evolution mechanisms of Rh-based catalysts

The HER in water electrolysis has been a focal point in energy catalysis, with the mechanism of catalysts varying significantly across different electrolyte environments. Rh-based catalysts exhibit distinct catalytic behaviors in acidic, alkaline and neutral media, influenced by the ionic composition and proton transport properties of the medium, which profoundly affect reaction pathways and kinetics.

Acidic media

In acidic electrolytes (e.g., H_2SO_4 or HCl solutions), the HER on Rh-based catalysts proceeds with protons (H^+) as the primary substrate, following the classical Volmer-Heyrovsky or Volmer-Tafel pathways^[46]. The reaction initiates with the Volmer step, where H^+ gains an electron on the catalyst surface to form H^* . This process relies on Rh's d-band electronic structure to maintain moderate adsorption energy for H^* —too strong adsorption blocks active sites, while too weak adsorption leads to rapid desorption of intermediates. The subsequent Heyrovsky step involves H^* combining with H^+ in the solution to generate H_2 , facilitated by the high proton concentration and efficient proton transport in acidic media, which accelerates kinetics. When H^* coverage is high, the Tafel step (direct recombination of two H^*) may dominate.

Alkaline media

The HER mechanism in alkaline environments (e.g., KOH solutions) is more complex, with water as the substrate and hydroxide (OH^-) participation introducing unique kinetic features^[46]. Water dissociation becomes the rate-determining step, featuring a significantly higher energy barrier than proton reduction in acidic media. Initially, water dissociates on the Rh surface into adsorbed OH^* and H^* , with the barrier of this step directly determining catalyst activity. The subsequent Volmer step generates H^* through proton supply from water or hydronium ions, while the Heyrovsky step releases H_2 via H^* reacting with water, regenerating OH^* . Notably, OH^- adsorption on Rh exhibits dual effects: moderate adsorption promotes water dissociation via an “ OH^- -assisted mechanism”, whereas excessive adsorption poisons active sites. Although Rh shows better oxidative stability in alkaline media than in acidic conditions, lattice distortion during long-term electrolysis can still cause activity decay, making interface engineering and structural regulation essential for enhancing stability.

Neutral media

HER in neutral media (e.g., phosphate buffer solutions (PBS) or natural water) combines features of both acidic and alkaline systems but faces dual challenges of low water dissociation and poor proton transport, leading to significantly slower kinetics^[51–53]. The reaction starts with direct water dissociation into H^* and OH^*

, requiring high energy due to the lack of high-concentration H^+ or OH^- assistance, thus necessitating specific active sites on the catalyst surface for water activation. Proton transfer relies on water cluster collaboration or trace H^+ in solution, acting as one of the rate-determining steps. In such media, optimizing catalyst hydrophilicity and proton transport pathways is crucial.

COMPUTATIONAL MODELS AND CATALYST DESIGN OF RH-BASED CATALYSTS

Computational models

In the theoretical research of the electrocatalytic HER, the synergistic application of the computational hydrogen electrode model (CHE), the potential-correction model, and the solvation-effect model can quantitatively predict the activity trend of catalysts and reveal the reaction mechanism^[54].

The computational model for Rh-based catalysts in the HER mainly predicts the catalytic activity through the synergistic simulation of the free energy of chemical adsorption (ΔG_{H^*})^[55], the potential effect, and the solvation effect. Based on the CHE, ΔG_{H^*} can be obtained by calculating the adsorption energy of hydrogen intermediates (H) on the catalyst surface using DFT, and combining it with the zero-point energy correction (ΔE_{ZPE}) and the entropy-change term ($T\Delta S_{\text{H}^*} \approx -0.20 \text{ eV}$)^[56]. Its ideal value should be close to 0 eV to achieve the balance between the Volmer step and the Heyrovsky/Tafel steps. To simulate the actual electrochemical environment, a potential model needs to be introduced. The influence of the applied potential (U) is incorporated into the calculation of ΔG_{H^*} through the charge-extrapolation method or work-function correction, which can be expressed as $\Delta G_{\text{H}^*}(\text{U}) = \Delta G_{\text{H}^*}(0) + e\text{U}$ ^[57], where the standard hydrogen electrode (SHE) is often used as a reference benchmark. In addition, the solvation effect corrects the interface charge distribution and adsorption energy through an implicit solvation model (such as Vienna *ab initio* Software Package (VASP))^[58] or an explicit water-molecule layer to more realistically reflect the catalytic behavior in an aqueous-solution environment. During the calculation, the Rh(111) surface or nanoclusters are usually used as models to optimize the configuration of H^+ at different adsorption sites (such as top sites, bridge sites, and vacancy sites)^[59], and the influence of the electronic structure on the activity is analyzed in combination with the-band center theory. However, the parameter sensitivity of the solvation model, the dynamic interface effect (requiring molecular dynamics simulation), and the strain and ligand effects of multi-component Rh-based catalysts (such as alloys or single-atom-dispersed systems) still need further optimization^[40,60–62]. These theoretical methods provide important guidance for the design of Rh-based HER catalysts, but need to be verified against experimental characterization to improve the prediction reliability.

Influence factor

The theoretical computational models for Rh-based HER catalysts are influenced by multiple factors including pH^[63], hydrogen coverage^[64] and applied electric field effects^[65]. These factors collectively regulate the catalytic activity and reaction mechanisms through complex interactions. Variations in pH directly affect the proton supply mechanism and double-layer structure at the electrode/electrolyte interface. In acidic media, HER primarily proceeds via H_3O^+ reduction, while in alkaline conditions, it relies on water dissociation processes. This difference leads to an increase in ΔG_{H^*} with rising pH, rendering the Volmer step the rate-limiting step in alkaline environments. Additionally, competitive adsorption of OH^- under high pH conditions further occupies active sites, necessitating explicit consideration in solvation models.

Changes in hydrogen coverage (θ_{H}) significantly alter ΔG_{H^*} values through site-blocking effects and H-H repulsion. Stronger hydrogen adsorption occurs at low coverage, but adsorption energy gradually increases with higher θ_{H} . This nonlinear relationship typically optimizes HER activity at moderate coverage levels. Notably, excessive θ_{H} not only inhibits further hydrogen adsorption but may also induce surface reconstruction or phase transitions, critically influencing catalyst stability. The applied electric field modulates catalytic performance by directly modifying ΔG_{H^*} and altering interfacial electronic structures,

cathodic potentials stabilize hydrogen adsorption, while anodic potentials weaken adsorption strength. Furthermore, strong electric fields induce solvent molecule alignment and interfacial charge redistribution, effects that require accurate description via self-consistent charge calculations or constant-potential DFT calculations.

Under practical reaction conditions, these factors often couple synergistically: OH⁻ in high-pH environments may oxidize under strong electric fields to block active sites, while high hydrogen coverage partially screens electric field effects on adsorption energy. Comprehensive understanding of these interactions demands integrating first-principles calculations with multiscale simulation approaches, validated by *in situ* spectroscopic techniques and microkinetic modeling. This integrated strategy enables the establishment of precise theoretical frameworks to guide the design and optimization of Rh-based HER catalysts.

Descriptors

Overview of descriptors

In the study of HER mechanisms for Rh-based catalysts using DFT, descriptors serve as critical bridges linking the microscopic structure of catalysts to their macroscopic catalytic performance. Through the analysis of descriptors, researchers can rapidly screen potential high-activity catalysts, gain deep insights into catalytic reaction mechanisms, and establish theoretical guidelines for the rational design of catalysts. Common descriptors relevant to Rh-based HER catalysts include ΔG_{H^*} , d-band center, and charge transfer quantities^[66].

Key descriptors and their applications

Hydrogen adsorption free energy (ΔG_{H^*}): ΔG_{H^*} is widely recognized as a critical descriptor for evaluating the activity of hydrogen evolution catalysts. Ideally, ΔG_{H^*} should approach zero^[67], indicating that the catalyst exhibits neither overly strong nor weak hydrogen adsorption, thereby facilitating efficient adsorption and desorption of hydrogen atoms on the catalyst surface to promote HER [Figure 2A and B]^[68,69]. Through DFT calculations, Fang *et al.*^[70] demonstrated that Rh single atoms (SAs) supported on specific substrates exhibit exceptional HER activity. They simulated the dispersion of various transition metal SAs on a C₃₀N₁₂Se₆H₁₂ matrix (denoted as TM@CNSeH) and evaluated hydrogen adsorption strength using ΔG_{H^*} as the descriptor. The resulting 2D and three-dimensional (3D) volcano plots revealed that HER activity peaks near the volcano summit. Notably, Rh SAs dispersed on the C₃₀N₁₂Se₆H₁₂ matrix exhibited the highest HER activity. This approach enables targeted design of efficient Rh-based HER catalysts by optimizing ΔG_{H^*} .

d-band center: The d-band center theory, proposed by Hammer and Nørskov^[71], provides a robust framework for understanding the adsorption and catalytic properties of transition metal catalysts. For Rh-based catalysts, the position of the d-band center governs the interaction strength between the catalyst and reactants. When the d-band center lies closer to the Fermi level, the interaction between the catalyst and hydrogen atoms strengthens, enhancing hydrogen adsorption^[72]. However, an excessively high d-band center may result in overly strong hydrogen adsorption, impeding hydrogen desorption. DFT calculations enable precise tuning of the d-band center by modifying the composition and structure of Rh-based catalysts. For example, in Rh-based single-atom catalysts, altering the coordination environment of the central Rh atom allows fine control of the d-band center [Figure 2C-E]^[69,70], thereby optimizing catalytic performance for HER.

Charge transfer amount: The charge transfer amount describes the degree of charge transfer between the catalyst and reactants during a catalytic reaction. In Rh-based hydrogen evolution catalysts, the amount of charge transfer is closely related to the activity of the catalyst.

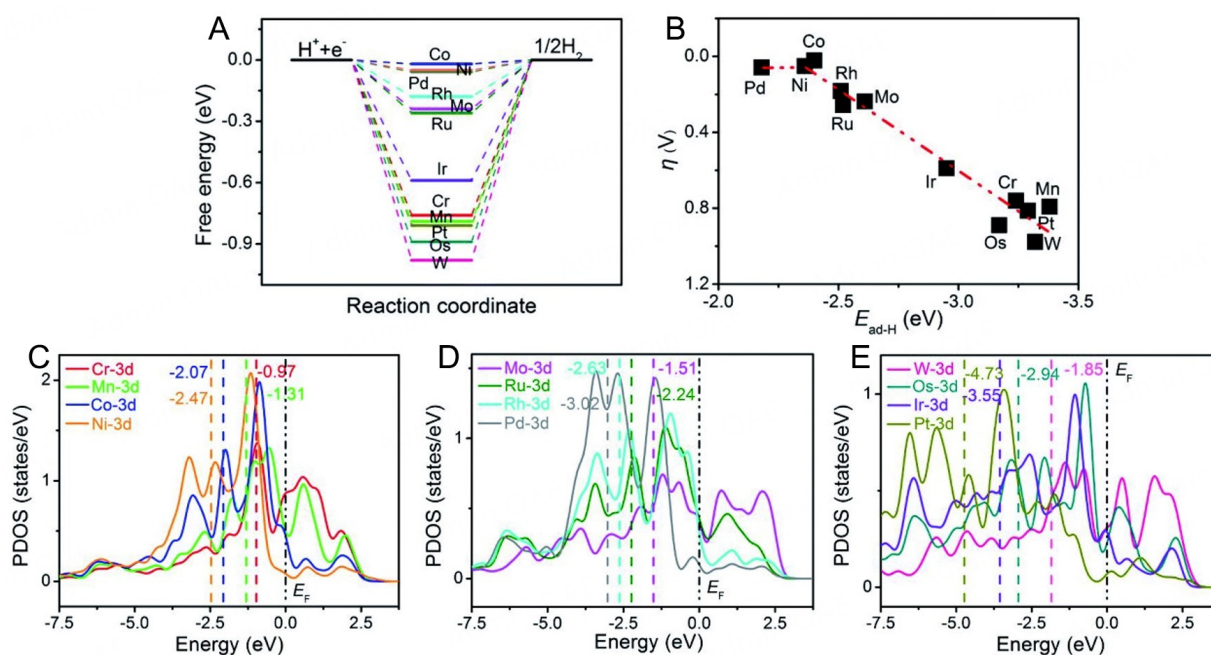


Figure 2. (A) Gibbs free energy diagram of the HER on TM-doped BNTs. (B) The volcano relationship between the E_{ad} of H and the overpotential of HER on TM-doped BNTs. (C-E) The partial density of states (PDOS) of the transition metal-doped BNTs. This figure is reproduced from Ref. [69] with permission. Copyright 2022, Royal Society of Chemistry.

Descriptor-guided catalyst design strategies

Composition modulation: Optimizing the catalytic performance of Rh-based catalysts by tuning their composition based on the relationship between descriptors and catalytic properties. For instance, to achieve ΔG_{H^+} close to zero, suitable metals can be alloyed with Rh, or specific dopants can be introduced into Rh-based catalysts. Additionally, selecting supports with appropriate electronic properties (e.g., carbon materials, metal oxides) can regulate the electronic structure and descriptors of Rh-based catalysts through interfacial interactions, thereby improving the catalytic performance^[18,73,74].

Structural optimization: Guiding the microstructural design of Rh-based catalysts using DFT calculations. Constructing Rh nanoparticles with specific crystallographic facets (e.g., high-index facets) adjusts the arrangement of surface atoms, modifies the d-band center position, and redistributes hydrogen adsorption sites, thereby optimizing HER performance^[75]. Research demonstrates that Rh nanoparticles with high-index facets exhibit unsaturated coordination of surface atoms, unique electronic structures, and enhanced adsorption properties, leading to significantly improved HER activity^[12]. Furthermore, designing nanoporous Rh-based architectures increases the specific surface area, maximizes active site exposure, and facilitates reactant adsorption and reaction^[76].

Interface engineering: Constructing efficient interfaces in Rh-based composite catalysts is a critical strategy for boosting catalytic performance^[77-79].

Interface engineering involves tailoring interactions at the atomic or molecular level between different components, which can include:

Heterostructure formation: Coupling Rh with metals, metal oxides/hydroxides, or carbon-based supports creates electronic interactions and charge redistribution at the interface, enhancing adsorption/desorption kinetics of reaction intermediates.

Strain and defect introduction: Interfacial strain or defects can induce lattice distortions and improved mass/charge transport, accelerating reaction dynamics.

Chemical bonding at interfaces: Covalent or coordination bonds between metal centers and heteroatom-doped carbon frameworks (e.g., Fe/Rh-anchored nitrogen-doped carbon hollow spheres (NCS)^[58]) can synergistically modulate electronic structures, generate additional active sites, and stabilize reaction intermediates.

These interfacial modifications influence catalytic performance by:

Tuning electronic structures: Adjusting the d-band center of Rh or the electronic density of carbon/oxide supports, thereby optimizing adsorption energies of key intermediates.

Generating synergistic effects: Combining the advantages of different materials (conductivity of carbon, activity of metals, stability of oxides) to achieve performance superior to individual components.

Enhancing stability and durability: Reducing catalyst aggregation, leaching, or surface reconstruction to improve long-term operation under harsh conditions.

Practically, descriptor-guided strategies link interfacial structural or electronic properties (e.g., strain, charge density, coordination number) with catalytic activity^[80–82], enabling rational design. Combining theoretical calculations with operando characterization facilitates identification of active sites and the precise role of interfaces, as demonstrated in Rh-carbon and Rh-metal oxide composites. Examples include tuning interfacial charge transfer in Rh-carbon composites to optimize hydrogen adsorption/desorption and introducing oxygen vacancies at Rh-oxide interfaces to promote water dissociation, thereby generating more reactive hydrogen species.

Machine learning-assisted catalyst design and screening

There are huge challenges in balancing catalytic activity (such as low overpotential), long-term stability (such as resistance to electrochemical corrosion), and cost control (reducing the loading of precious metal Rh). By integrating multi-source data (such as experimentally measured overpotential, Tafel slope, cyclic voltammetry data, as well as the ΔG_{H^+} calculated by DFT, surface electron density of states, energy barriers at alloying sites, *etc.*), machine learning can construct a cross-scale “structure-performance” prediction model, providing key theoretical guidance for catalyst design. The workflow of high-throughput computational screening is shown in Figure 3^[83]. Therefore, machine learning has opened up an efficient and accurate data-driven path for the design and screening of Rh-based HER catalysts. For example, a model based on a graph neural network (GNN) can analyze the regulation mechanism of the local coordination environment (such as Rh-N₄, Rh-S₃, *etc.*) of Rh single-atom catalysts (Rh-SACs) on ΔG_{H^+} , while Gaussian process regression (GPR)^[84] is suitable for predicting the synergistic catalytic effect of Rh-based alloys (such as Rh-Fe, Rh-Mo) with small sample data. To address the bottleneck of scarce data for Rh-based catalysts, transfer learning can leverage the known structure-activity relationships of Pt-based or transition metal sulfide catalysts and apply them to the Rh-based system^[83,85,86]. Complemented by an active learning strategy to generate high-value data in a targeted manner, it significantly reduces the dependence on experimental/computational resources. In addition, multi-objective optimization algorithms (such as Non-dominated Sorting Genetic Algorithm II (NSGA-II), Bayesian optimization) can simultaneously balance the objectives of activity, stability, and cost, guiding the design of innovative systems such as core-shell structures^[87,88], high-entropy alloys (diluting the Rh content)^[47,89], or support interface engineering (such as Rh/MXene, Rh/N-doped carbon)^[90]. Studies have shown that the Rh-Co dual-atom catalyst screened

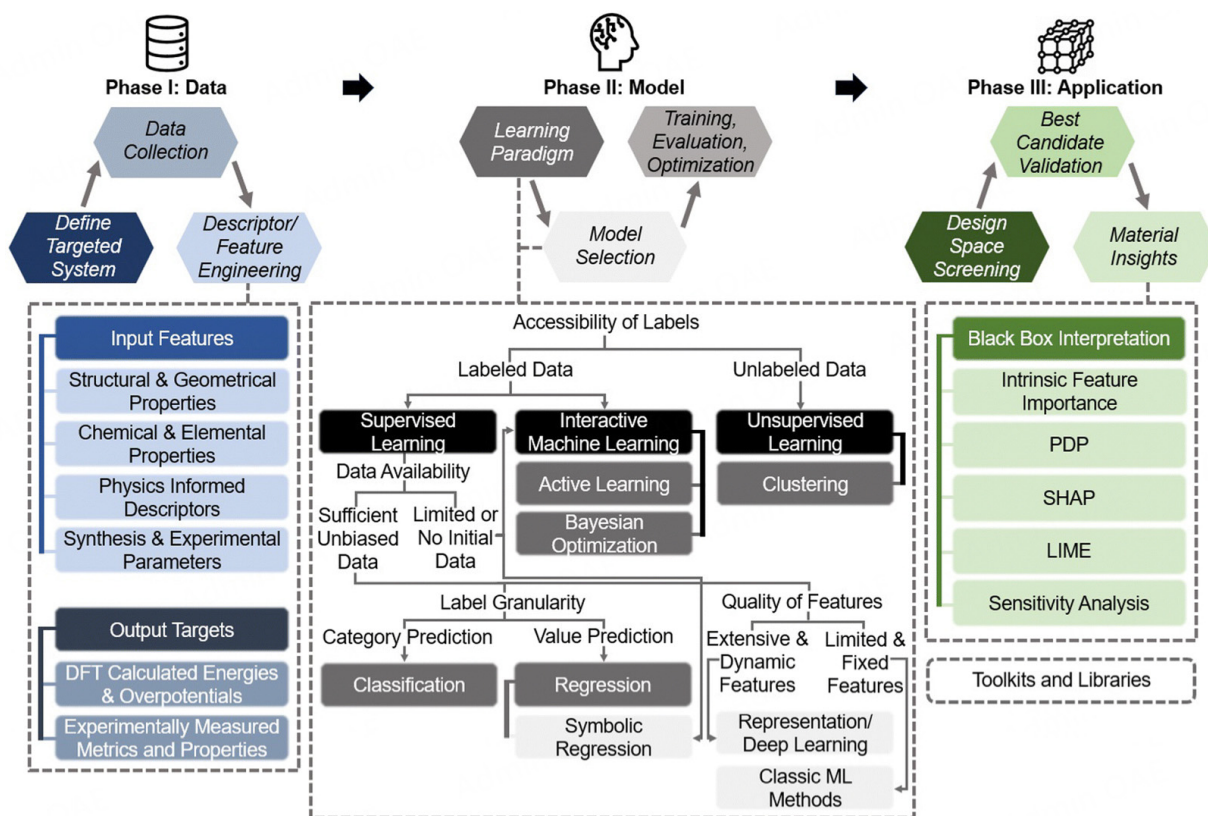


Figure 3. Framework for machine learning-assisted electrocatalyst design. Reproduced with permission, Copyright 2024, Royal Society of Chemistry^[83].

by machine learning has an overpotential^[83], and its cyclic stability is increased by more than 5 times compared with pure Rh, verifying the feasibility of the data-driven strategy. In the future, a closed-loop design system that integrates cross-scale modeling (from atomic adsorption to macroscopic reaction kinetics), automated high-throughput experimental platforms (robot synthesis and *in-situ* characterization), and sustainability assessment (life cycle analysis) will accelerate the transformation of Rh-based HER catalysts from laboratory exploration to industrial application, providing key technical support for the large-scale preparation of green hydrogen and the achievement of the carbon neutrality goal.

In conclusion, in-depth research on the descriptors of Rh-based hydrogen evolution catalysts using DFT calculations, combined with catalyst design based on these descriptors, provides theoretical support for developing high-performance Rh-based catalysts. These efforts can offer new insights and help advance HER technology.

ADVANTAGES OF RH-BASED CATALYSTS FOR HER

Activity aspects

Rh has unique advantages in catalytic applications for the HER. Although it has been studied less compared to Pt or Ru, it exhibits significant performance potential under specific conditions. The following includes the main advantages of Rh in HER.

Moderate hydrogen adsorption energy (ΔG_{H^*})

The hydrogen adsorption energy is a key parameter determining hydrogen evolution activity. An ideal catalyst should have a hydrogen adsorption energy (ΔG_{H^*}) close to thermodynamic neutrality ($\Delta G_{H^*} \approx 0$ eV)

to achieve rapid equilibrium between adsorption and desorption. Evidence from DFT calculations: The ΔG_{H^*} of the (111) crystal plane of pure Rh is approximately -0.12 eV, which is slightly stronger than that of Pt ((111) $\Delta G_{\text{H}^*} \approx -0.09$ eV). However, it can be further optimized through alloying or nanostructure design. For example, in the Rh_3Cu_1 alloy^[91], electron transfer from Cu to Rh leads to an upshift of the Rh d-band center, thereby optimizing the ΔG_{H^*} and facilitating both adsorption and desorption of hydrogen intermediates. The synergistic electronic modulation between Rh and Cu effectively balances the adsorption strength of H^* , significantly lowering the energy barrier for HER. As a result, the defect-rich RhCu nanotubes with the Rh_3Cu_1 phase exhibit superior HER performance across a wide pH range, achieving a small overpotential of 8 mV at $10 \text{ mA}\cdot\text{cm}^{-2}$ in alkaline conditions and remarkable overall water-splitting activity.

Excellent electrochemical active surface area (ECSA)

An excellent Electrochemical Active Surface Area (ECSA) is a key performance metric for Rh-based HER catalysts because it reflects the actual number of accessible active sites rather than just geometric area. Nanostructuring (nanowires, concave/tetrahedral nanoparticles, porous supports) and clean-surface synthesis routes dramatically increase the ECSA of Rh materials^[37,92,93], leading to higher mass activity and lower overpotentials. For example, ultrathin wavy Rh nanowires show extremely large ECSA and correspondingly high mass activities^[93], while concave/curved Rh nanoparticles and Rh nanocrystals supported on porous graphdiyne (GDY) exhibit substantially enhanced double-layer capacitance (C_{dl})-derived ECSA and superior HER performance in acid^[37].

Efficient water dissociation ability (in alkaline conditions)

In the alkaline HER, the dissociation of water molecules (Volmer step) is the rate-controlling step of the reaction, and Rh-based catalysts can significantly reduce the water dissociation energy barrier. DFT calculations systematically reveal the intrinsic advantages of Rh-based catalysts in the HER from the aspects of electronic structure and energy evolution. The unique d-electron configuration of Rh makes its d-band center close to the Fermi level and moderately distributed. It can effectively adsorb hydrogen intermediates (H^*) while avoiding the increase in desorption energy barrier caused by overly strong adsorption, thus occupying a nearly optimal activity interval in the “volcano curve”. Through the alloying strategy, DFT simulations show that the introduction of inexpensive metals can induce lattice strain and electron redistribution in Rh, synergistically regulating the surface charge environment and significantly optimizing the ΔG_{H^*} to be close to the thermoneutral value. In addition, the interface engineering of Rh-based catalysts, through the electronic coupling between the support and the active center, can simultaneously enhance the charge transfer efficiency and inhibit surface oxidation and corrosion, providing a theoretical basis for high stability.

Stability aspects

Rh-based catalysts can undergo surface reconstruction under reaction conditions, forming dynamic active sites and avoiding activity decay caused by intermediate poisoning. DFT dynamic simulation: In the alkaline HER, metastable Rh-OH species (adsorption energy ≈ -0.3 eV) will form on the surface of Rh nanoparticles. Through periodic DFT simulations, it is found that these species can be rapidly regenerated through a water-assisted proton exchange mechanism ($\text{Rh-OH} + \text{H}_2\text{O} \rightarrow \text{Rh-H}^* + \text{OH}^-$), maintaining a highly active surface. Lattice distortion effect^[94]: The grain boundaries of ultrafine Rh nanoparticles (~ 2 nm) induce lattice strain. DFT calculations confirm that the d-band broadening in the strained region enhances the adsorption-desorption cycle stability of H^* (activity decay rate $< 5\%/100$ h). In summary, Rh-based catalysts are significantly superior to traditional Pt-based or transition metal-based catalysts in terms of hydrogen evolution activity due to their moderate ΔG_{H^*} , high ECSA, efficient water dissociation ability, and dynamic stability. Combining rational design based on DFT calculations (such as alloying and interface engineering)

can further break through the activity limit and promote their application in industrial water electrolysis devices.

Economic aspects

Although Rh is one of the most expensive materials among precious metals (the price of Rh was approximately ten times that of Pt in 2023), its potential low-cost substitution in HER catalysis can be achieved through multi-dimensional strategies^[35,60,95,96]. In alkaline conditions, the performance advantages of Rh-based catalysts are particularly significant. To further reduce the absolute amount of Rh used, nanostructure engineering is crucial. By designing Rh nanowires, Rh metallene, or ultrathin two-dimensional (2D) materials^[76,97,98], the density of active sites can be increased compared with traditional particulate catalysts, reducing Rh loading in a single cell from the milligram to the microgram level. For instance, by anchoring Rh nanocrystals on porous GDY, a minimal Rh loading of only ~0.244 wt% is sufficient to achieve excellent HER performance^[37]. DFT studies indicate that the high-activity stepped surfaces and GDY-induced d-band modulation of active sites effectively accelerate both water dissociation and hydrogen recombination. As a result, this catalyst delivers a low overpotential of 65 mV at a high current density of 1,000 mA cm⁻², demonstrating that even with ultralow Rh usage, high catalytic efficiency can be maintained. Such a combination of ultralow noble-metal content, high activity, and structural stability highlights a promising strategy to reduce Rh consumption while preserving HER performance, offering clear economic advantages for large-scale hydrogen production. Moreover, the recovery of precious metals plays a pivotal role in determining the total cost of ownership. Currently, Rh recovery rates can exceed 95%^[99]. By combining ultralow Rh loadings, high intrinsic activity, excellent long-term stability, and closed-loop metal recovery, Rh-based catalysts emerge as a viable solution for hydrogen production in high-value or harsh-environment applications.

TYPES OF RH-BASED HYDROGEN EVOLUTION CATALYSTS

Rh-based nanomaterials exhibit great potential in the electrochemical HER due to their unique electronic structures and excellent catalytic properties. Through component regulation, structural design, and interface engineering, significant progress has been made in Rh-based hydrogen evolution catalysts in terms of reducing overpotential, improving stability, and enhancing intrinsic activity. In recent years, researchers have further optimized Rh-based hydrogen evolution catalysts from the aspects of atomic-level modification^[58,100], as well as modification of graphene-like^[76,101], cluster-like^[6], and nanoparticle-type Rh-based materials^[33,37], alloying^[91,95], composite structure design^[87,102], and support design^[98,103] [Figure 4].

Atomic-level modification

In the research of Rh-based hydrogen evolution catalysts, single-atom catalysts and heteroatom-doped catalysts have shown unique performance advantages, providing new ideas and methods for improving the activity, selectivity, and stability of the catalysts.

Single-atom Rh-based hydrogen evolution catalysts

Single-atom Rh catalysts precisely anchor isolated Rh atoms on the surface of the support, constructing highly uniform active centers. This unique atomic-level dispersion structure not only avoids the agglomeration problem of traditional nanocatalysts but also achieves precise regulation of the electronic structure through the strong interaction between the metal and the support. Under the action of the coordination environment, the electrons in the d orbitals of Rh atoms are rearranged, making the electron cloud distribution reach the optimal state, thus significantly enhancing the catalytic activity and stability. This atomic-level dispersion structure endows single-atom Rh catalysts with extremely high atomic utilization efficiency. Different from traditional nanoparticles where only surface atoms participate in the reaction, the single-atom configuration makes each Rh atom an effective active site. Through the rational design of the support material, excellent catalytic performance can be achieved with an extremely low loading of precious metals, providing new ideas for the development of resource-saving catalysts.

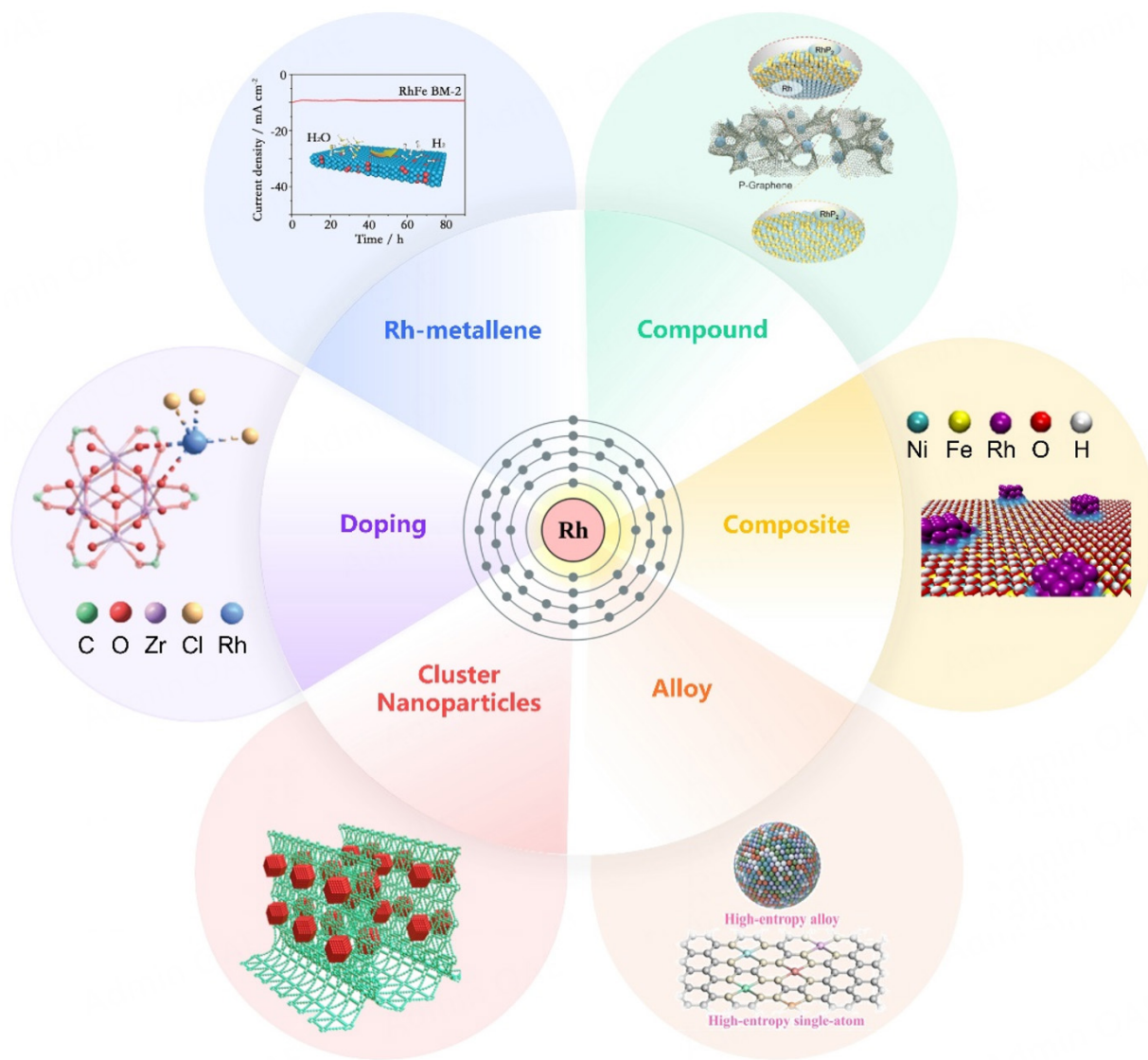


Figure 4. Classification of Rh-based HER catalysts^[37,95,100–103]. Doping is reproduced from Ref.^[100] with permission. Copyright 2022, Wiley. Rh-metallene is reproduced from Ref.^[101] with permission. Copyright 2022, Wiley. Compound is reproduced from Ref.^[103] with permission. Copyright 2023, Wiley. Composite is reproduced from Ref.^[102] with permission. Copyright 2019, American Chemical Society. Alloy is reproduced from Ref.^[95] with permission. Copyright 2024, Springer. Cluster is reproduced from Ref.^[37] with permission. Copyright 2022, Springer.

The core advantage of single-atom Rh catalysts lies in their unique coordination environment and electronic structure. The chemical bonding between the support and Rh atoms not only stabilizes the active center but also optimizes the adsorption behavior of reaction intermediates through the electron transfer effect. This precise regulation at the atomic scale enables the catalyst to maintain high activity while exhibiting excellent anti-poisoning ability and environmental adaptability, opening up new avenues for catalytic applications under complex conditions. For example, Dong *et al.*^[100] prepared a Rh-SAC with high accessibility by loading it on the metal nodes of metal-porphyrin-based PCN metal-organic frameworks (MOFs, PCN-224) as supporting material. Notably, the PCN-Rh15.9/Ketjenblack (KB) catalyst with a high Rh content (15.9 wt%) showed excellent hydrogen evolution activity. It could reach a current density of 10 mA cm⁻² at a low overpotential of 25 mV and had a mass activity of 7.7 A mg⁻¹ Rh at an overpotential of 150 mV, far superior

to the commercial Rh/C catalyst [Figure 5A–C]. Various characterizations indicated that the metal nodes with O/OH_x in MOFs stabilized the Rh species, which is crucial for high loading and good activity^[100]. In addition, the catalyst also showed satisfactory performance and excellent long-term stability in acidic seawater, indicating its broad application prospects in hydrogen production from seawater. Logeshwaran *et al.*^[40] used electrospinning technology to achieve the spontaneous integration of Rh SAs on carbon nanofibers embedded with TiO₂ [Figure 5D and E]. The obtained Rh-TiO₂/carbon nanofibers (CNF) showed great potential as an innovative and effective electrocatalyst for HER. DFT analysis highlighted the key role of the binary-type Rh SAs promoted by the TiO₂ sites. In a single-cell setup, Rh-TiO₂/CNF reached an industrial-grade current density of 1 A cm⁻² and exhibited extended durability of 225 h. Doan *et al.*^[73] engineered a composite catalyst by anchoring Rh SAs onto interconnected Mo₂C nanosheets, which were tightly integrated within a 3D Ni_xMoO_y nanorod array framework. This unique structure synergistically modulated the electrocatalytic properties of Mo₂C, enabling broad pH adaptability and exceptional durability^[73]. Remarkably, the catalyst delivered HER performance rivaling that of commercial Pt/C. Under a current density of 10 mA cm⁻², it exhibited impressively low overpotentials of 31.7 mV in acidic, 109.7 mV in neutral, and 95.4 mV in alkaline media, along with favorable Tafel slopes of 42.4, 51.2, and 46.8 mV dec⁻¹, respectively [Figure 5F]^[73].

The core design concept of single-atom Rh catalysts lies in precisely anchoring individual Rh atoms onto the surface of the support to achieve atomic-level dispersion and electronic structure modulation. By selecting supports with abundant metal sites or heteroatom coordination, the Rh SAs can be effectively stabilized while enabling synergistic regulation of the interfacial electronic structure.

Heteroatom-doped Rh-based hydrogen evolution catalysts

Regulation of Electronic Structure and Active Sites: Heteroatom doping is to introduce other elements (such as transition metals, non-metallic elements, *etc.*) into Rh-based catalysts to change the electronic structure and the properties of active sites of the catalysts^[18]. Different heteroatoms have different electronic structures and chemical properties, and their interactions with Rh atoms will lead to changes in the electron cloud density and electronic states around Rh atoms. For example, when some non-metallic elements with high electronegativity (such as N, P, S, *etc.*) are doped into Rh-based catalysts, these elements will attract the electrons around Rh atoms, causing the d-band center of Rh atoms to shift, thus adjusting the adsorption energy for hydrogen atoms^[18]. In addition, the introduction of heteroatoms may also form new active sites on the catalyst surface, or change the structure and properties of the original active sites, further promoting the HER.

The synergistic effect between heteroatoms and Rh atoms is one of the key factors for the performance improvement of heteroatom-doped catalysts. In some cases, heteroatoms can act as co-catalysts and participate in the HER together with Rh atoms, improving the activity and selectivity of the reaction. For example, in Rh-based alloy catalysts, the doped transition metal atoms can form an alloy phase with Rh atoms, changing the electronic structure and surface properties of the alloy, thereby enhancing the ability to adsorb and activate hydrogen. In addition, the doping of heteroatoms can also improve the stability of the catalyst, inhibit the agglomeration and loss of Rh atoms^[75], and extend the service life of the catalyst. This is because heteroatoms can form stable chemical bonds with Rh atoms, restricting the migration and aggregation of Rh atoms, thus maintaining the active structure of the catalyst.

In conclusion, single-atom and heteroatom doping are effective strategies for optimizing the performance of Rh-based hydrogen evolution catalysts. By regulating the electronic structure, active sites, and atomic utilization efficiency of the catalysts, *etc.*, they provide important approaches for the development of

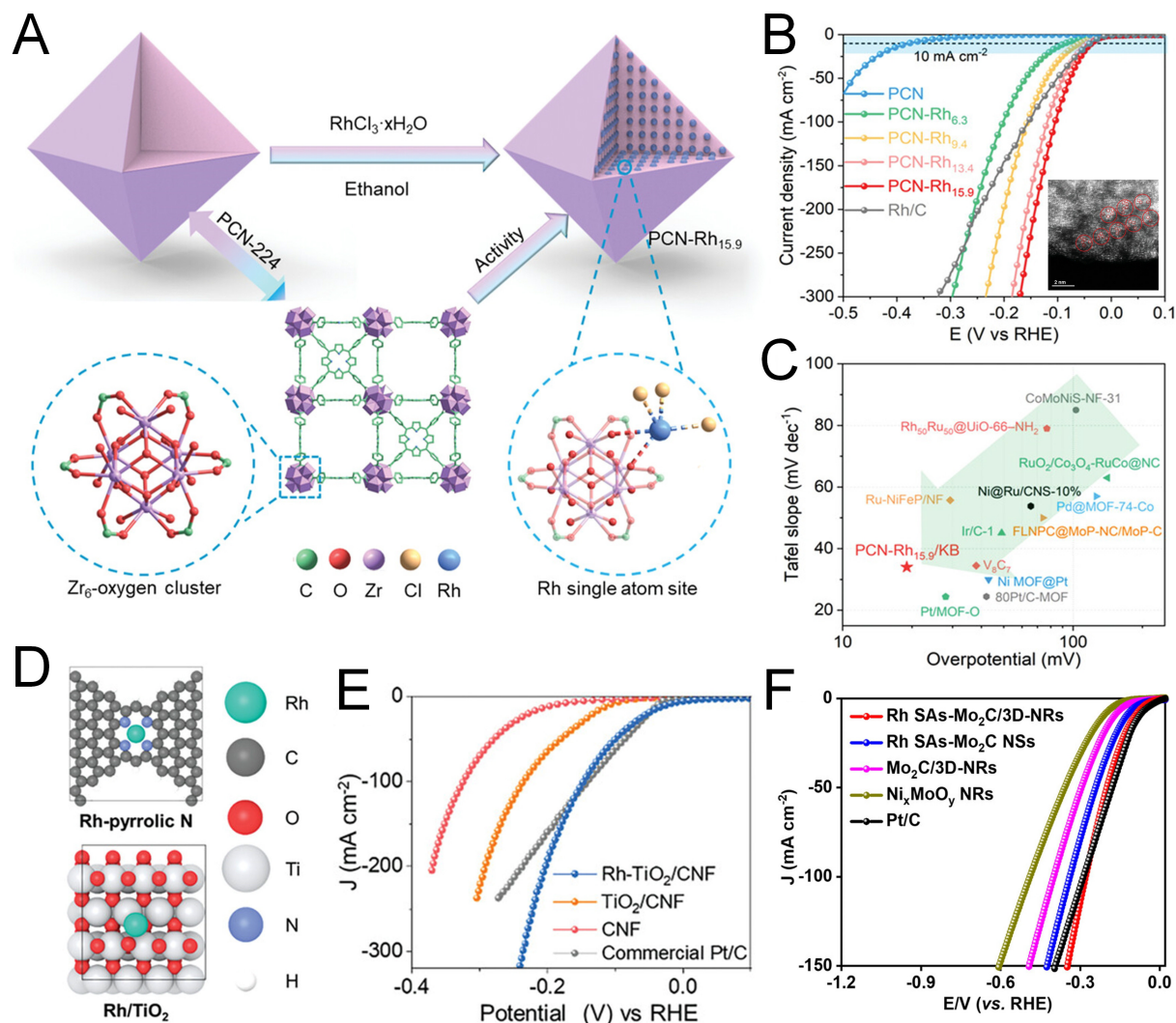


Figure 5. (A) Synthesis process and the coordination environment of single Rh atom on metal nodes of PCN. (B) LSV curves of various catalysts in 0.5 M H_2SO_4 at 1,600 rpm. Inset: HAADF-STEM images of PCN-Rh_{15.9}. (C) Comparative analysis of overpotentials at 10 mA cm^{-2} and Tafel slopes of PCN-Rh_{15.9}/KB with different reported HER catalysts, (A-C) are reproduced from Ref.^[100], with permission, Copyright 2023, Wiley. (D) DFT-optimized atomic models depicting the geometry of each catalyst configuration. (E) LSV curves of Rh-TiO₂/CNF, TiO₂/CNF, Pt/C, and CNF. (D and E) are reproduced from Ref.^[40], with permission, Copyright 2024, Wiley. (F) Electrocatalytic HER performance in alkaline medium (1.0 M KOH): iR-compensated LSV curves for Ni_xMoO_y nanorod arrays (NRs), Rh SAs-Mo₂C NSs, Mo₂C/3D-NRs, Rh SAs-Mo₂C/3D-NRs, and Pt/C. Reproduced from Ref.^[73], with permission, Copyright 2023, Wiley.

high-performance hydrogen evolution catalysts. Future research can further explore the mechanisms of single-atom and heteroatom doping in depth, as well as how to achieve more efficient catalyst design and preparation. Table 1 presents the key performance parameters of recently reported single-atom Rh-based HER catalysts used in acidic and alkaline environments.

Rh-metallene catalysts

Metallene is a 2D material composed of a single layer or a few atomic layers of metal atoms, typically arranged in a periodic lattice structure, analogous to graphene^[106]. Due to the behavior of delocalized electrons, metallene exhibits excellent electronic transport properties. Moreover, the undercoordinated surface atoms confer high catalytic activity, making metallene highly active in catalytic reactions^[107]. Rh-metallene (Rhene) materials, as a new type of catalytic material, have the following main advantages: Firstly, their unique molecular structure endows Rhene with high surface activity and electron transfer

Table 1. Summary of the HER activity of monoatomic Rh-based materials used in acid and alkaline solutions

Catalyst	Activity (mV@mA cm ⁻²)		Stability	Ref.
	Acid	Alkaline		
Rh-TiO ₂ /CNF		24@10	225 h@1 A cm ⁻²	[40]
Rh SAs-Mo ₂ C/3D-NRs	31.7@10 74.6@50	95.4@10 199.4@50	40 h@50 mA cm ⁻²	[73]
PCN-Rh _x	25@10		50 h@10 mA cm ⁻²	[100]
Rh-Co ₃ S ₄ /CoO _x NTs	56.1@10 124.2@50		40 h@50 mA cm ⁻²	[60]
NiRh-Cu NA/CF		12@10 123@150	30 h@50 mA cm ⁻²	[104]
Cu/Rh(SAs) + Cu ₂ Rh(NPs)/GN	8@10		500 h@10, 50 and 100 mA cm ⁻²	[59]
Rh@NG	29@10	33@10	25 h@25 mA cm ⁻²	[105]
Fe/Rh-anchored NCS	24@10			[58]

efficiency, thus showing significant advantages in the HER. Secondly, this type of material usually has good stability and can work stably for a long time under strongly alkaline or strongly acidic conditions, meeting the requirement of the durability of catalysts for the water electrolysis reaction. Thirdly, the molecular structure of Rhene can be optimized in terms of performance through functional modification, and it has a high degree of controllability. In addition, this type of material can achieve efficient hydrogen and oxygen evolution at a low overpotential, making it an ideal choice in the fields of clean energy production. However, Rhene also has some significant disadvantages. Firstly, their preparation process is complex and the cost is high, which limits their large-scale application. Secondly, the catalytic activity of this type of material may be limited under certain specific conditions, and further optimization is needed to adapt to a wider range of reaction environments. Finally, since the catalytic mechanism of Rhene has not been fully elucidated, there are still theoretical bottlenecks in improving its performance and expanding its functions. In conclusion, although Rhene has broad application prospects in water electrolysis, achieving high efficiency at low cost, along with a deeper understanding of the catalytic mechanism, remains a key research direction for the future.

Jiang *et al.*^[15] synthesized a novel Ir@Rhene heterojunction electrocatalyst by epitaxially confining ultra-small and low-coordinated Ir nanoclusters on an ultrathin Rh metal, accompanied by the formation of Ir/IrO₂ Janus nanoparticles [Figure 6A-C]. It showed excellent alkaline HER activity, with an overpotential of only 17 mV at 10 mA cm⁻² [Figure 6D]. The dual-site synergy between IrO₂ and the Ir/Rh interface facilitates interfacial hydrogen spillover, effectively mitigating steric hindrance at active centers and thereby enhancing HER kinetics under alkaline conditions. Mao *et al.*^[76] developed a partially hydroxylated Rh metallene (Rh/RhOOH metallene) featuring a porous, ultrathin framework with abundant defects and heterogeneous interfaces for ethylene glycol-assisted seawater electrolysis [Figure 6E-H]. During the electrocatalytic process, the unique interplay of RhOOH redox behavior and ethylene glycol-driven electroreduction induces dynamic *in-situ* reconstruction of the catalyst, generating additional active Rh species. This reconstruction enriches the active sites and optimizes surface catalytic reactions. Owing to its distinctive metallene morphology and the Rh/RhOOH heterostructure, the material demonstrates outstanding HER activity.

Table 2 presents the key performance parameters of recently reported graphene-like Rh-based HER catalysts used in acidic and alkaline environments.

Rhene catalysts achieve an organic integration of high activity, excellent stability, and high atomic utilization

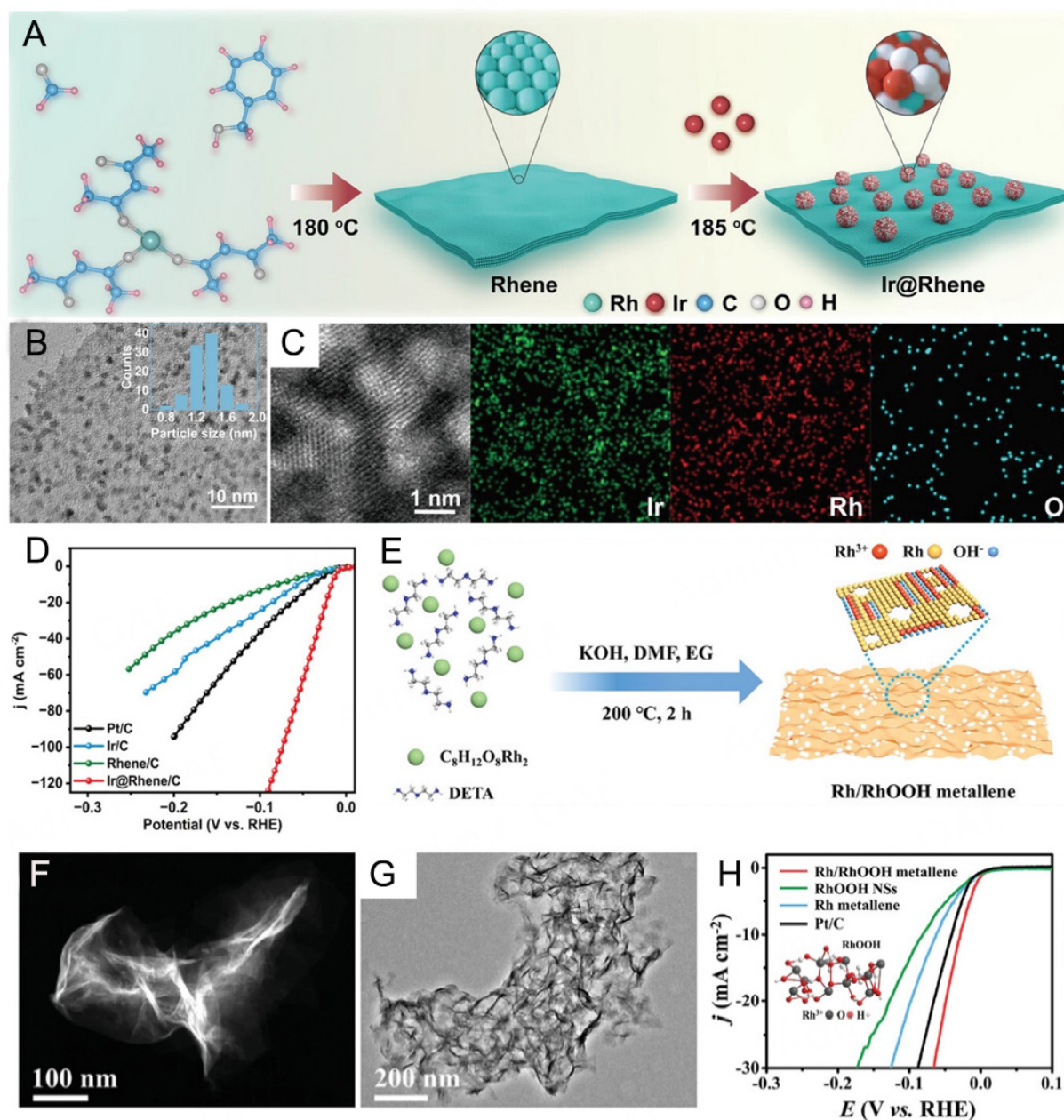


Figure 6. (A) Schematic diagram of the synthesis of Ir@Rhene heterostructure, (B) typical low-magnification TEM image (inset: size distribution of the nanocluster), (C) HAADF-STEM-EDS elemental mapping images of Ir@Rhene heterostructure. (D) Polarization curves of Ir@Rhene/C, Rhene/C, and commercial Pt/C and Ir/C. (A–D) are reproduced from Ref. [165], with permission, Copyright 2023, Wiley. (E) Schematic diagram of the synthesis process for the Rh/RhOOH metallene. (F) Low and high-magnification HAADF-STEM image and (G) low-magnification TEM image of the Rh/RhOOH metallene. (H) HER polarization curves for various electrocatalysts. Inset: local ball-and-stick model of RhOOH. (E–H) are reproduced from Ref. [166], with permission, Copyright 2022, Wiley.

through the rational design of 2D atomic-layer structures, electronic state modulation, and interface engineering. Their performance enhancement mainly arises from the optimized ΔG_{H^*} , rapid charge transfer, and strain/defect-induced activation effects. Rhene provides a new design paradigm for noble-metal-based 2D electrocatalysts and exhibits broad application prospects in future hydrogen energy conversion systems.

Clusters and nanoparticles of Rh-based catalysts

In the Rh-based hydrogen evolution catalyst system, cluster and nanoparticle catalysts play an important role

Table 2. Summary of the HER activity of metal alkene-type Rh-based materials used in acid and alkaline solutions

Catalyst	Activity (mV@mA cm ⁻²)		Stability	Ref.
	Acid	Alkaline		
Ir@Rhene/C		17@10	50 h@10 mA cm ⁻²	[15]
Rh/Pd metallene		59@10	20 h@10 mA cm ⁻²	[108]
Pt-Rhene		37@10	50 h@10 mA cm ⁻²	[1]
Rh-O-W	7@10	8@10	48 h@10 mA cm ⁻²	[5]
Rh/RhOOH metallene		29@10	20 h@10 mA cm ⁻²	[76]
I-Rh metallene		38@10	20 h@10 mA cm ⁻²	[109]
Rh/Fe BM-2		24.4@10 34.6@100	90 h@10 mA cm ⁻²	[101]

in the HER due to their unique physical and chemical properties, and their performance optimization strategies have also attracted much attention.

Cluster-type Rh-based catalysts

Rh clusters are usually composed of several to dozens of Rh atoms, with a size generally in the range of 1–3 nm. Due to their extremely small size, the proportion of surface atoms is extremely high, resulting in a large number of atoms in a state of coordination unsaturation. In a cluster composed of 13 Rh atoms, compared with bulk Rh atoms, Rh₁₃ clusters adopt a more compact geometric configuration, exhibit stronger s-d orbital hybridization, and possess a higher d-electron occupancy^[110]. Moreover, nearly all atoms in the cluster reside on or near the surface, resulting in electronic structures and active-site properties that are markedly distinct from those of larger nanoparticles or bulk Rh. Through high-resolution transmission electron microscopy (HRTEM) combined with theoretical calculations, it has been found that the atoms on the surface of the cluster can adsorb and activate hydrogen atoms in a special way, providing an efficient catalytic active center for the HER^[16]. The strong interaction between the atoms inside the cluster also affects its overall electronic structure. Compared with SAs, the electron delocalization phenomenon among the atoms in the cluster is more obvious, and the synergistic effect of electrons makes the adsorption and activation ability of the cluster for reactant molecules different from that of SAs or larger nanoparticles^[111,112]. This unique electronic structure endows the cluster-type Rh-based catalyst with unique catalytic performance in the HER.

The size of the cluster has a crucial influence on its catalytic performance. As the size of the cluster decreases, the proportion of surface atoms further increases, the number of active sites increases, and the adsorption energy of hydrogen atoms also changes. Zheng *et al.*^[6] constructed Rh nitride nanoclusters (Rh_xN-NC) supported on N-doped carbon using a simple molten urea method [Figure 7A and B]. The uniformly distributed Rh_xN clusters exhibited optimized water binding and water electrolysis effects, achieving excellent HER performance in a full pH environment. The optimized Rh_xN-NC catalyst exhibits remarkable activity, requiring minimal overpotentials of only 8 mV in 0.5 M H₂SO₄ and 12 mV in 1.0 M KOH to achieve a current density of 10 mA cm⁻² [Figure 7C and D]. In a related study, Wang *et al.*^[41] developed Rh clusters anchored on a molybdenum oxycarbide (MoOC) support to facilitate efficient hydrogen evolution for water splitting applications [Figure 7E]. Combined experimental and theoretical investigations revealed significant charge transfer from Rh to the MoOC substrate, leading to favorable modulation of the d-band center, water adsorption properties, and hydrogen binding energy—all contributing to enhanced intrinsic HER performance. Moreover, the presence of interstitial carbon and oxygen atoms within the MoOC matrix plays a pivotal role in accelerating water dissociation during the HER process. Notably, at an overpotential of 100 mV, the Rh/MoOC catalyst delivered a hydrogen evolution rate over 40 times greater than the

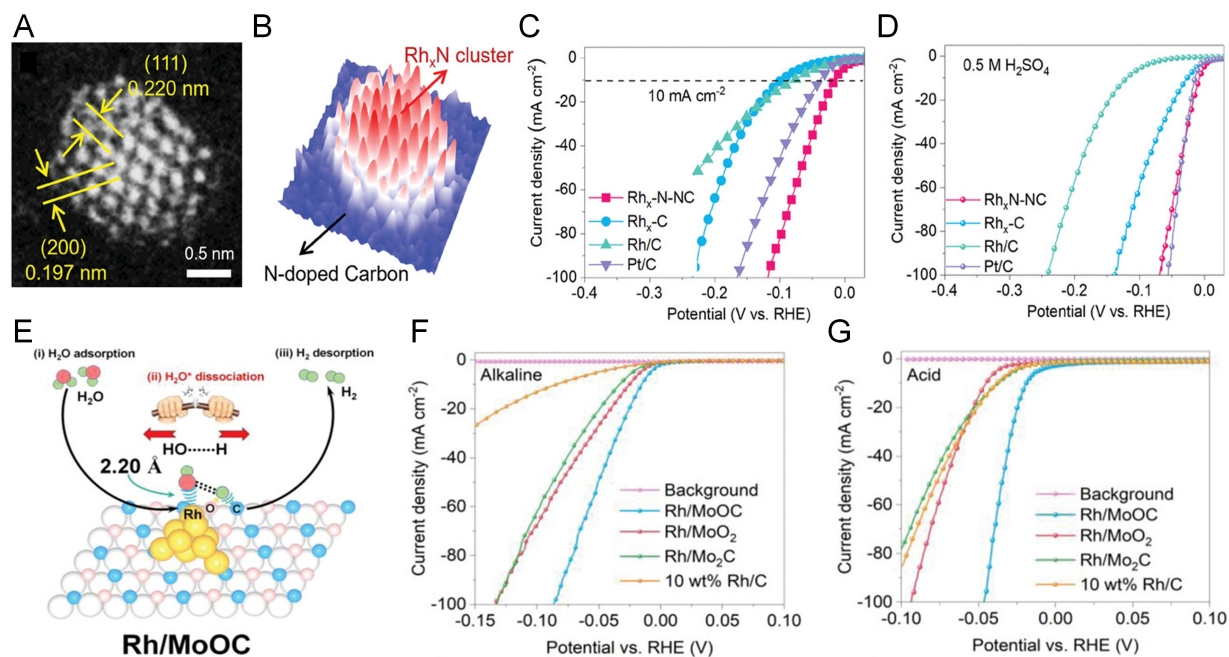


Figure 7. (A) HAADF-STEM images of Rh_xN-NC at different magnifications. (B) 3D intensity surface plot is shown for the Rh nanocluster in a. HER polarization curves of different catalysts in (C) 1.0 M KOH and (D) 0.5 M H₂SO₄. (A–D) are reproduced from Ref. [61], with permission, Copyright 2023, Wiley. (E) Schematic illustration for alkaline HER by efficiently splitting the HO–H bond on Rh–C sites of MoOC with the O atom-tuned microenvironment and electronic structure. Performance of Rh/MoOC catalysts and control samples in a three-electrode configuration in (F) 1 M KOH and (G) 0.5 M H₂SO₄ at room temperature. (E–G) are reproduced from Ref. [41], with permission, Copyright 2022, Wiley.

commercial Rh/C, demonstrating its superior catalytic efficiency [Figure 7F and G].

Rh cluster catalysts occupy an intermediate position between single-atom catalysts and nanoparticles, combining the advantages of both: they retain the high utilization of atomic-level active sites while possessing a relatively stable structural framework. Through size control, electronic structure engineering, and interface coupling, they achieve a synergistic integration of high activity, superior stability, and high atomic utilization. Their performance enhancement primarily arises from optimized hydrogen adsorption energy, synergistic electronic effects, and stable metal-support interactions. Rh clusters provide an important design strategy for developing novel, highly efficient noble-metal electrocatalysts that bridge the gap between single-atom and nanoscale systems.

Nanoparticle-type Rh-based catalysts

The size of nanoparticles has a significant impact on their catalytic performance. Nanoparticle-type Rh-based catalysts typically range from 3 to 100 nm. Smaller nanoparticles have a larger specific surface area, more surface atoms, and a higher density of active sites, which benefits the progress of the HER. For example, Rh nanoparticles with a size of about 3 nm have a lower initial hydrogen evolution potential and a larger hydrogen evolution current density in the acidic HER^[113]. As the size of the nanoparticles increases, the specific surface area decreases, the proportion of internal atoms increases, and the catalytic activity gradually decreases. Water electrolysis across a wide pH range represents a promising approach for hydrogen production, necessitating the development of highly stable and active electrocatalysts for the HER. Cao et al.^[114] developed a novel nanocomposite consisting of polyallylamine-functionalized ultrafine Rh nanoparticles (PA@Rh uNPs) uniformly anchored on 3D graphene aerogel (GA). This was achieved through a straightforward surface adsorption-chemical reduction method conducted at ambient temperature. As evidenced by experimental data, the PA@Rh uNPs/GA nanocomposite exhibits a 3D porous structure, with

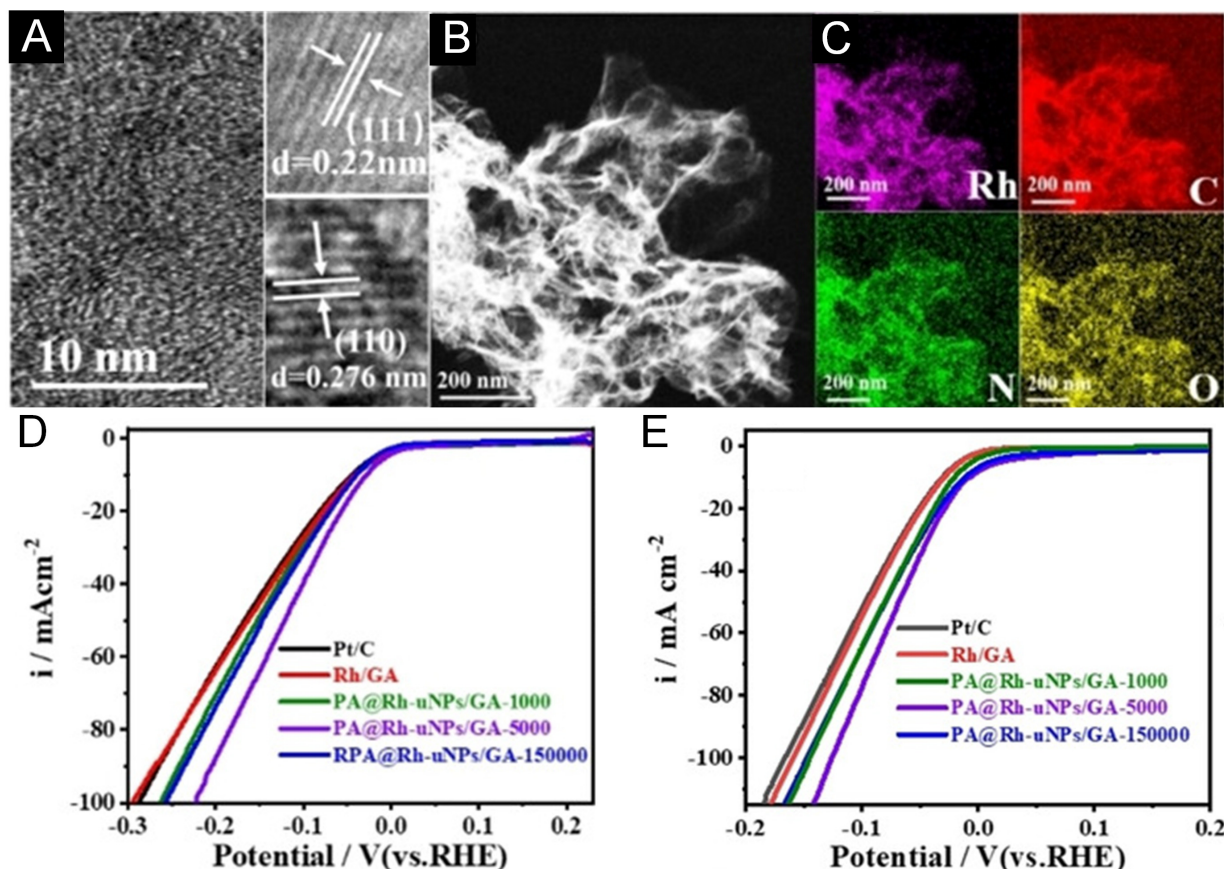


Figure 8. (A) High-resolution TEM image of PA@Rh uNPs/GA-5000 nanocomposites. (B) STEM image and (C) corresponding EDX elemental distribution maps for PA@Rh-uNPs/GA-5000. (D and E) HER polarization curves of various electrocatalysts-including PA@Rh-uNPs/GA-5000, PA@Rh-uNPs/GA-1000, PA@Rh-uNPs/GA-150000, Rh/GA nanocomposites, and commercial 20% Pt/C-measured in (D) 0.1 M HClO₄ and (E) 0.1 M KOH electrolytes, respectively. This figure is reproduced from Ref.^[114] with permission. Copyright 2021, Wiley.

PA@Rh uNPs of 1.3 nm in size being uniformly distributed across the GA surface [Figure 8A-C]. Electrochemical investigations revealed that the molecular weight of polyallylamine significantly influences the HER activity of the PA@Rh uNP-based nanocomposite. Notably, the optimized PA@Rh uNPs/GA nanocomposite containing 10% Rh by mass demonstrated superior HER performance compared to a commercial 20% Pt/C electrocatalyst over a broad pH range [Figure 8D and E].

Different crystal planes of Rh nanoparticles exhibit distinct atomic arrangements and electronic structures, leading to varying activities for the HER. Common crystal planes include (111), (100), and (110); among these, the (111) plane has a relatively dense atomic arrangement and moderate hydrogen adsorption energy, resulting in higher HER activity^[75]. By controlling the synthesis conditions of the nanoparticles, their crystal plane composition and exposure ratio can be regulated. For example, using a specific surfactant-assisted synthesis method can make the Rh nanoparticles preferentially expose the (111) crystal plane, thereby improving the hydrogen evolution performance of the catalyst^[115].

Surface modification of Rh nanoparticles is an important strategy for optimizing their hydrogen evolution performance. Surface modification can be achieved by changing the chemical environment and electronic structure of the nanoparticle surface. Modification can also be carried out by depositing other metal atoms or compounds on the surface of the Rh nanoparticles. For example, depositing a small amount of platinum atoms on the surface of the Rh nanoparticles to form a Rh-Pt alloy shell structure^[87]. In this structure, the

presence of platinum atoms changes the electronic structure and the interaction between atoms on the surface of the Rh nanoparticles, synergistically promoting the HER. Experimental results show that the catalytic activity and stability of the Rh nanoparticles modified with the Rh-Pt alloy in the acidic HER are significantly improved compared with those of the pure Rh nanoparticles.

Rh nanoparticle HER catalysts achieve high activity, superior stability, and high surface atomic utilization through nanoparticle size and morphology control, interface engineering, alloying, and surface modification. Their performance enhancement primarily arises from the abundance of low-coordinated active sites, optimized electronic structure, and synergistic interface effects. Rh nanoparticles provide an important design strategy for developing efficient and scalable noble-metal HER catalysts.

Table 3 summarizes the key performance parameters of the recently reported cluster-type and nanoparticle-type Rh-based HER catalysts for acidic and alkaline environments.

Compounds-type Rh-based catalysts

In recent years, researchers have significantly improved the catalytic performance of Rh-based phosphides in water electrolysis by regulating their crystal structures, surface activities, and electronic properties^[14,136,137]. Especially under alkaline conditions, this type of material exhibits excellent stability and efficient hydrogen evolution ability, providing a new technical pathway for clean energy production. However, its practical application still faces key challenges such as further improvement of catalytic activity, optimization of material synthesis processes, and control of large-scale preparation costs. Future research should focus on the development of new synthesis methods and the design of multifunctional materials, with the aim of more efficiently achieving the goal of hydrogen production through water electrolysis. Xin *et al.*^[138] reported the one-step synthesis of polyhedral-shaped and morphology-controllable Rh phosphide (Rh₂P) nanoparticles via high-temperature pyrolysis under an inert atmosphere. In 0.5 M H₂SO₄ and 1 M KOH electrolytes, the overpotentials of the polyhedral Rh₂P nanoparticles at 10 mA m⁻² are 12.6 mV and 10.5 mV, respectively, which are even lower than those of Pt/C^[138]. Theoretical calculations show that the {200} plane of Rh₂P nanoparticles has the highest catalytic activity among the {200}, {111} and {220} planes, with the lowest free energy of hydrogen adsorption. The extensive exposure of the {200} crystal plane is beneficial for achieving the high catalytic activity of Rh₂P^[138].

Rh oxides, such as Rh₂O₃, *etc.*^[74,139], exhibit certain catalytic activity. Their crystal structure and electronic properties confer a unique mechanism of action for the HER. During the catalytic process, surface oxygen atoms can promote water dissociation by interacting with water molecules, providing a hydrogen source for subsequent hydrogen evolution steps. Simultaneously, transitions between different oxidation states of Rh ions facilitate electron transfer, further promoting HER activity. Kundu *et al.*^[74] reported the synthesis of Rh-Rh₂O₃ nanoparticles/N-doped carbon composites (Rh-Rh₂O₃-NPs/C) for HER [Figure 9A-C]. This catalyst can achieve a current density of 10 mA cm⁻² with overpotentials of only 63 mV and 13 mV in alkaline and acidic media [Figure 9D-F], respectively, and its HER activity is approximately 2.2 times and 1.43 times that of the industrial Pt/C catalyst, respectively. For the HER in an alkaline medium, water is adsorbed and dissociated at the Rh₂O₃ sites, and H_{ads} is formed at the adjacent Rh sites. The recombination of H_{ads} leads to the formation of hydrogen molecules.

Rh sulfides, such as RhS, Rh₂S₃, *etc.*^[140], have been studied for HER catalysis. The sulfur atoms in these sulfides can modulate the electronic structure of Rh, optimizing hydrogen adsorption and desorption properties. Compared with oxides, sulfides may exhibit better stability under certain acidic conditions, reducing catalyst corrosion and deactivation during the reaction. Moreover, their surface structure facilitates hydrogen adsorption and recombination, thereby enhancing HER efficiency.

Table 3. Summary of the HER activity of Rh-based materials of cluster type and nanoparticle type used in acid and alkaline solutions

Catalyst	Activity (mV@mA cm ⁻²)		Stability	Ref.
	Acid	Alkaline		
Rh/SNG		13@10	100 h@500 mA cm ⁻² (70 °C)	[19]
Rh/GNPs	76@10		5 h@2 mA cm ⁻²	[90]
Pd-Rh/MoS ₂	46@10		30 h@10 mA cm ⁻²	[116]
Electro-deposited Rh electrodes	168@onset	339@onset	48 h@2 V	[117]
Au _{0.25} Rh _{0.75}	105@10		25 h@10 mA cm ⁻²	[118]
Cs ₃ Rh ₂ I ₉ /NC-R	25@10		50 h@10 mA cm ⁻²	[33]
Rh _x N-NC	8@10	12@10	10 h@10 mA cm ⁻²	[6]
0.15Co-NCNFs-5Rh	18@10	13@10	30 h@10 mA cm ⁻²	[34]
Co-Rh ₂		2@10	10 h@10 mA cm ⁻²	[12]
Rh@Pt ₂ L		5@10	5 h@10 mA cm ⁻²	[13]
B-Rh@NC	43@10	26@10	10 h@20 mA cm ⁻²	[32]
Rh-NiAl LDH/NF		14@10	70 h@38 mA cm ⁻²	[119]
sRhNPs	27.4@10			[120]
Pt ₃ NiRh NFs	7@10 18@50			[97]
N-Rh/CA		65@10 210@100		[121]
Rh ₂ /C		3@10 79@100	5 h@10 mA cm ⁻²	[113]
Rh/MoOC		15@10	80,000 s@10 mA cm ⁻²	[41]
PA@Rh uNPs/GA	16@10	28@10	100,000 s@10 mA cm ⁻²	[114]
MRNs	29.4@10		20 h@10 mA cm ⁻²	[122]
RhNiP MNs	15@10	36@10	20 h@10 mA cm ⁻²	[123]
Rh/DNA-1	105@10 194@50		10 h@15 mA cm ⁻²	[124]
Rh/NHCSs	10@10	6@10	12 h@10 mA cm ⁻²	[17]
4.2 Rh-CN	13@10	46@10	12 h@10 mA cm ⁻²	[98]
Rh NCs/NHCAs		7@10 48@100	6 h@10 mA cm ⁻²	[125]
Rh ⁰ /TiO ₂ -2000	37@10			[126]
Rh(nP)/nC	44@2			[127]
P-Rh/C		11@10		[128]
hollow Rh nanoparticles	28.1, 32.6, 37.6@10, 20, 40		3,500 s@10 mA mg ⁻¹	[129]
Rh/SiQD/CQD	36@10		23 h@10 mA cm ⁻²	[130]
Rh@NPCP	23@10	20@10		[131]
Rh/Ni@NCNTs	45@10	14@10		[132]
Rh-Pt-B		31@10		[11]
Rh NCs		32@10	6 h@10 mA cm ⁻²	[133]
Rh NP/C		7@10 12@20 22@50 36@100	20 h@10 and 20 mA cm ⁻²	[35]
W-Rh/C	57@10		2 h@10 mA cm ⁻²	[92]
Rh-NSs		42@10	6,000 s@5 mA cm ⁻²	[36]
Rh/N-CBs		77@10	6,000 s@1.7V	[45]
0.5Rh-GS1000	40@10	25@10	10 h@15 mA cm ⁻²	[39]
29.1 wt% Rh/SiNW	44@100			[2]

Rh/F-graphene-2	46@10	50,000 s@10 mA cm ⁻²	[134]
Rh NP/PC	21@10		[38]
Rh NSs	43@10	5 h@5 mA cm ⁻²	[135]

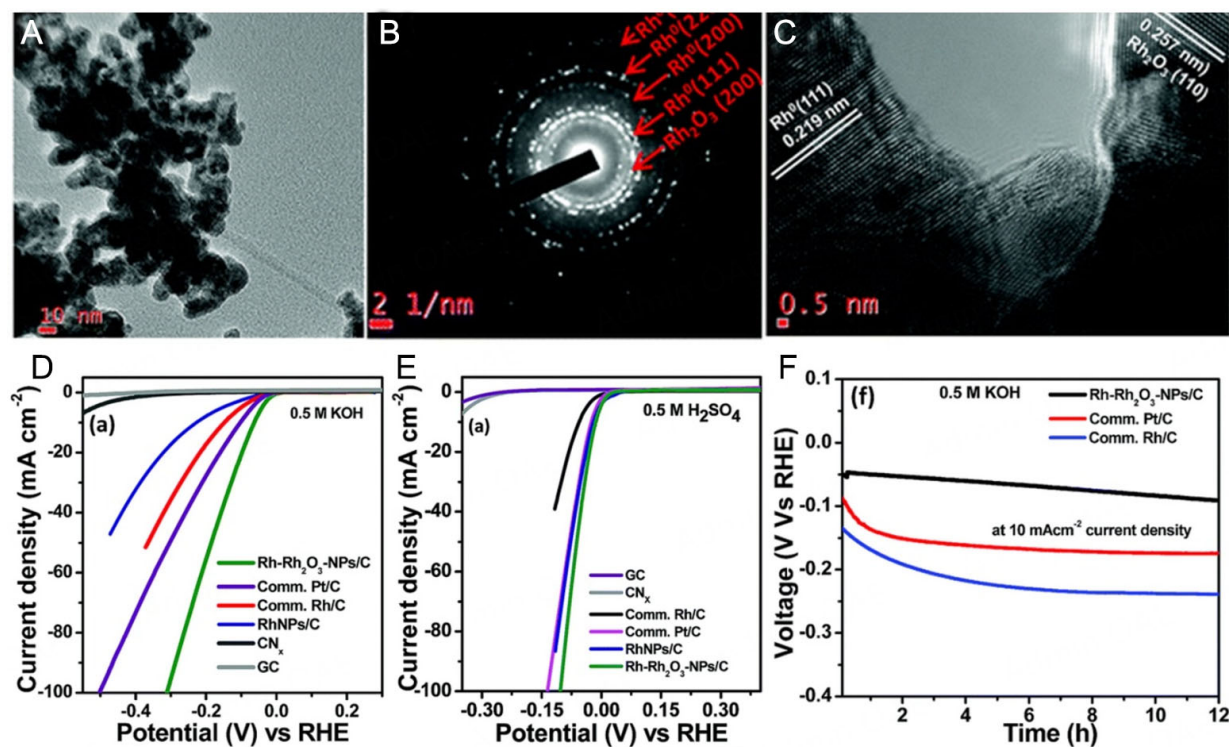


Figure 9. (A) TEM, (B) SAED and (C) HRTEM images of the Rh-Rh₂O₃-NPs/C composite. (D) HER curves of Rh-Rh₂O₃-NPs/C, comm. Pt/C, comm. Rh/C, RhNPs/C, CN_x and GC in 0.5 M KOH (E) 0.5 M H₂SO₄. (F) Chronopotentiometric stability of Rh-Rh₂O₃-NPs/C, Pt/C and Rh/C at 10 mA cm⁻². This figure is reproduced from Ref. [74] with permission. Copyright 2018, Royal Society of Chemistry.

Nitrides usually have high hardness and stability, and can maintain good catalytic performance under some harsh reaction conditions, which helps to improve the service life of the catalyst. Meanwhile, the introduction of nitrogen atoms will change the distribution of the electron cloud of Rh, making the electronic structure of the catalyst surface more conducive to the adsorption and activation of hydrogen.

Compounds-type Rh-based HER catalysts achieve a synergistic integration of high activity, superior stability, and high atomic utilization through chemical composition tuning, crystal structure and surface coordination engineering, interface coupling, and defect/doping modulation. Their performance enhancement mechanisms mainly include optimized H⁺ adsorption/desorption, synergistic electronic structure regulation, interface- and defect-induced activity, and enhanced environmental adaptability. Compound-type catalysts provide important design strategies for developing efficient, durable, and resource-efficient Rh-based HER catalytic systems.

Table 4 shows the key performance parameters of the recently reported Rh-based compound HER catalysts for acidic and alkaline environments.

Alloys-type Rh-based catalysts

As an emerging multi-component catalytic material, Rh-based high-entropy alloy materials exhibit unique application potential in HER during water electrolysis. Due to the significant advantages of their

Table 4. Summary of the HER activity of Rh-based compound used in acid and alkaline solutions

Catalyst	Activity (mV@mA cm ⁻²)		Stability	Ref.
	Acid	Alkaline		
Rh ₂ P@NPG-150	30.4@10	57.3@10	9 h@10 mA cm ⁻²	[141]
RhFeP		28@10	24 h@10 mA cm ⁻²	[142]
NiRh ₂ Sb		121@10		[143]
CuRh ₂ Sb		145@10		
Rh(OH) ₃ /CoP	12@10	13@10	70 h@10 mA cm ⁻²	[7]
RhP ₂ /Rh@NPG	9@10	21.3@10	50 h@10 mA cm ⁻² 24 h@50 mA cm ⁻²	[103]
Rh ₂ P	11.7@10	10.3@10	40 h@10 mA cm ⁻²	[137]
a/c-RuB		39@10	20 h@10 mA cm ⁻²	[144]
Rh ₂ P-900	12.6@10	10.5@10	35 h@15 mV/13 mV	[138]
Rh ₂ P	21@50	14@50		[145]
R-RhFeP ₂ CX-CNT	15@10	53@10	7 h@130/100 mA cm ⁻²	[146]
Rh(OH) ₃ /NiTe		21@10	75 h@10 mA cm ⁻²	[147]
Rh ₁₅ /NSC YSS		13.5@10	10 h@10 mA cm ⁻²	[148]
Ni _{2-x} Rh _x P		66.2@10	10 h@0.085 V	[149]
p-Rh/Fe-Ni ₃ S ₂ /NF		108@100	50 h@100 mA cm ⁻²	[150]
Ni _{1.66} Rh _{0.34} P/C	149@10			[151]
RhTe ₂ /C		47@10	10 h@10 mA cm ⁻²	[152]
Rh ₂ P{200}	22@10	23@10	10 h@1 A cm ⁻²	[153]
Rh-Pt-B		31@10		[11]
Rh ₂ SbNBs/C		39.5@10	20,000 s@0.1 V	[154]
Co _{0.25} Rh _{1.75} P		58.1@10	10 h@12.5 mA cm ⁻²	[155]
RhRu-MPSs		25@10		[156]
Co _{0.75} Rh _{1.25} P	90.5@10			[157]
Rh ₂ P-N/P-CC	4@20			[158]
	44@100			
	71.5@200			
	115@400			
RP-500	14.3@10	4.3@10	60,000 s@10 mA cm ⁻²	[159]
Rh/Rh ₂ P-NFAs	13.4@10	19.5@10		[160]
RhSe ₂	49.9@10	81.6@10		[161]
RhRh ₃ Se ₄ /C	32@10	29@10	50 h@10 mA cm ⁻²	[162]
Rh-Rh ₂ P@C	24@10	37@10		[163]
Rh ₂ P/NPC	40@10	17@10	10 h@10 mA cm ⁻²	[164]
SLNP		14@10	50 h@10 mA cm ⁻²	[139]
		46@50		
Rh ₂ S ₃ -ThickHNP/C	122@10			[140]
Rh ₁₇ S ₁₅ /C	340@20			[165]
Rh ₂ P-1@CB/Nafion	1.5@5	1@5		[145]
RhNiP MNs	15@10	36@10	20 h@10 mA cm ⁻²	[123]
RhP _x @NPC	22@10	69@10	10 h@10 mA cm ⁻²	[166]
Ru _x P/NPC	19@10		20 h@-50 mV	[136]
w-Rh ₂ P NS/C	15.8@10	18.3@10		[14]
Rh ₂ P	14@10	30@10	60,000 s@10 mA cm ⁻²	[167]
Rh ₃ Pb ₂ S ₂ /C	87.3@10			[168]

Rh ₂ P@NC	9@10	10@10	10 h@10 mA cm ⁻²	[169]
Rh ₂ P/C	5.4@5			[170]
RhPd-H NPs		36.6@10	4 h@10 mA cm ⁻²	[3]
Rh-Ag/SiNW-2	120@10			[171]
Rh-Rh ₂ O ₃ -NPs/C	13@10	63@10	12 h@10 mA cm ⁻²	[74]
Rh-Au-SiNW-2	62@10			[172]

multi-metallic composition, such as excellent mechanical properties, corrosion resistance, and efficient electron transfer characteristics, Rh-based high-entropy alloys show high catalytic activity and stability in the electrochemical water splitting reaction. Researchers have further improved their catalytic performance in alkaline media by regulating the alloy composition ratio, surface modification, and multiphase structure design^[62,173,174]. Especially in the HER process, this type of material shows a low overpotential and excellent long-term stability^[175,176], providing a new technical means for efficient water splitting. However, although Rh-based high-entropy alloy materials perform well in laboratory research, there are still many challenges in their large-scale preparation cost, verification of stability in practical applications, and performance optimization. Future research directions should focus on developing economically viable preparation methods, deeply understanding their catalytic deactivation mechanism, and further exploring their practical applicability in industrial water splitting, with a view to achieving more efficient and large-scale clean hydrogen production. Luo *et al.*^[47] synthesized micro-strain modulated high-entropy alloy nanoparticles (IrRuRhMoW HEA NPs) in the sub-2 nanometer range, which served as an excellent HER catalyst. Under alkaline conditions, the current density reached 10 mA cm⁻² at an overpotential of only 28 mV [Figure 10A and B]. Ultraviolet photoelectron spectroscopy, DFT calculations, and electrochemical characterizations speculated that due to the enhancement of the ligand effect and micro-strain effect, the d-band center of the HEA nanoparticles decreased and the oxygen affinity increased, enabling appropriate regulation between H_{ad} and OH_{ad} adsorption to promote hydrogen electrocatalysis. This work demonstrates a new strategy for achieving multi-intermediate binding energy optimization in high-performance energy conversion catalysis by introducing unique local micro-strains in HEA nanocatalysts.

Rh-transition metal alloys commonly include Rh-Fe, Rh-Co, Rh-Ni and other alloys. After transition metals form alloys with Rh, they will change the electronic structure and crystal structure of the alloy. For example, in the Rh-Co alloy^[177], the addition of Co atoms will affect the electronic structure around Rh atoms, causing changes in the alloy's ability to adsorb and activate hydrogen. This change may lead to the alloy having better catalytic performance in the HER^[177]. Compared with pure Rh catalysts, it can reduce the overpotential of the HER and increase the reaction rate.

Rh-precious metal alloys commonly include Rh-Pt, Rh-Au, *etc.* Alloys formed between precious metals have good catalytic activity and stability. Taking the Rh-Pt alloy as an example^[178], the addition of platinum can further improve the electron migration ability of the alloy and optimize the adsorption-desorption equilibrium of hydrogen on the catalyst surface. Since platinum itself is also an excellent hydrogen evolution catalyst, after forming an alloy with Rh, the synergistic effect of the two can give full play to their respective advantages, showing high hydrogen evolution catalytic activity in both acidic and alkaline electrolytes.

Rh-rare earth metal alloys formed by Rh and rare earth metals (such as Ln, La, Tm, *etc.*) have also received widespread attention^[179,180]. Rare earth metals have special electronic configurations and chemical properties. Adding them to Rh-based alloys can improve the surface properties and stability of the alloys. For instance, in Rh₃Ln intermetallic^[179], the alloying process induces an upward shift of the d-band center and facilitates electron transfer from Ln to Rh, thereby optimizing the adsorption and dissociation energies of H₂O molecules.

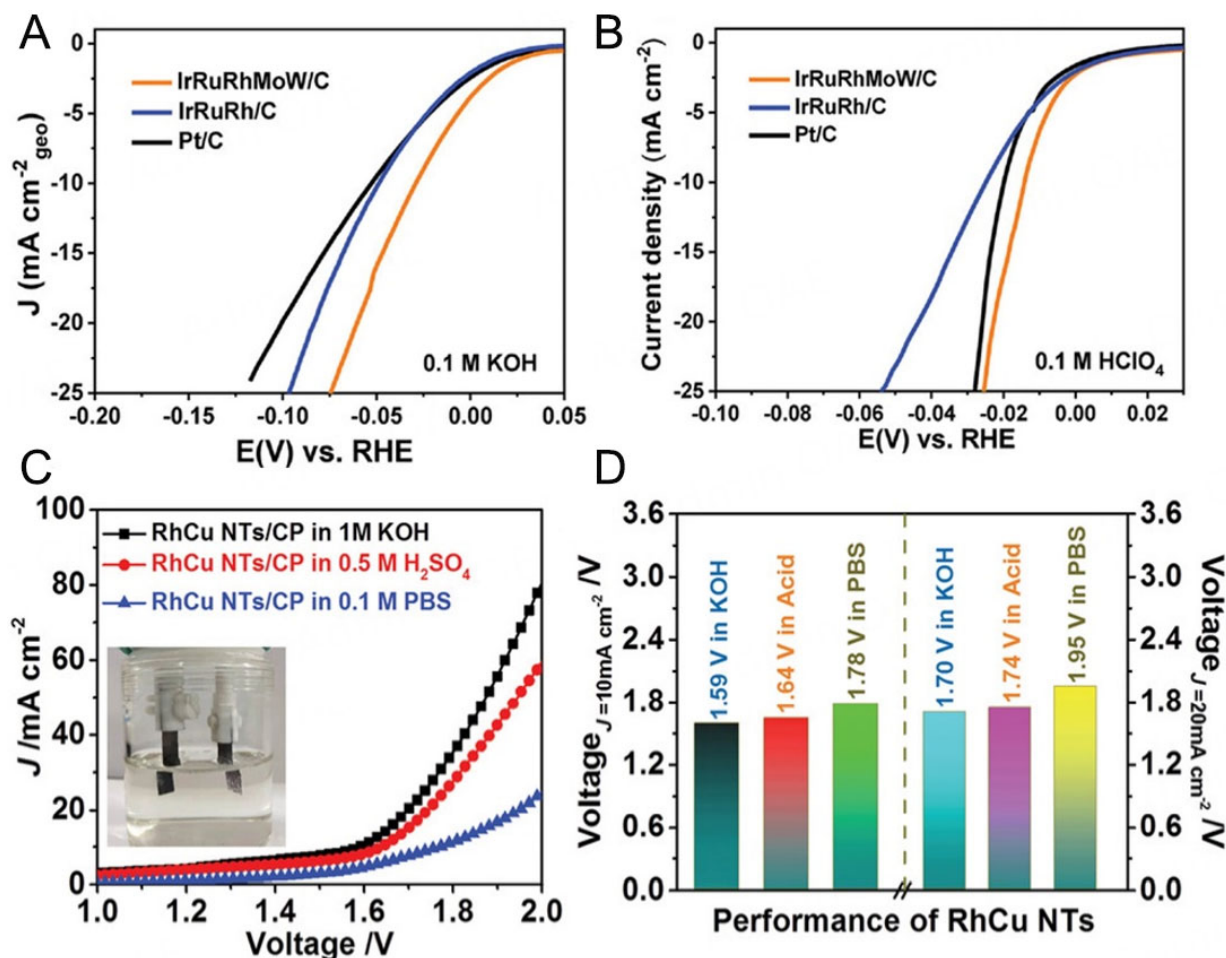


Figure 10. HER polarization curves of IrRuRhMoW/C, IrRuRh/C, and Pt/C in (A) 0.1 M KOH and (B) 0.1 M HClO_4 . (A and B) are reproduced from Ref.^[47], with permission, Copyright 2024, Wiley. (C) LSV curves for overall water splitting in a two-electrode system with RhCu nanotubes employed as both the anode and cathode. Inset: Photograph of the two-electrode system. (D) Comparison of voltage requirements at current densities of 10 and 20 mA cm^{-2} across various pH levels. (C and D) are reproduced from Ref.^[91], with permission, Copyright 2020, Wiley.

Precisely controlling the proportion of each element in the alloy is the key to optimizing the performance of Rh-based alloy catalysts. By changing the alloy composition, the electronic structure and crystal structure of the alloy can be adjusted, and then its catalytic performance for the HER can be optimized. For example, in the Rh-Ni alloy, when the atomic ratio of Rh to nickel reaches a certain value, a special electronic structure will form on the alloy surface, making the adsorption energy of hydrogen on the catalyst surface moderate, which is conducive to both the adsorption and activation of hydrogen and the desorption of hydrogen, thus improving the efficiency of the HER. Usually, the method of combining experimental screening with theoretical calculation is adopted to determine the optimal alloy composition. Cao *et al.*^[91] successfully synthesized RhCu nanotubes with abundant structural defects by the mixed solvent method, which showed excellent activity and stability for the HER and the oxygen evolution reaction in all pH value ranges. In particular, under alkaline, acidic, and neutral conditions, only 8, 12, and 57 mV are required, respectively, to achieve a current density of 10 mA cm^{-2} for HER [Figure 10C and D]. DFT calculations revealed that exposing the appropriate composition of the highly active Rh_3Cu_1 alloy phase through acid etching is the key to improving the electrocatalytic performance^[91], because it weakens the adsorption free energy of atomic oxygen and hydrogen and promotes the dissociation of water molecules. In addition, structural defects can

also improve the catalytic performance, as the adsorption of reactants can be greatly enhanced.

Furthermore, selecting an appropriate preparation method is crucial for obtaining high-performance Rh-based alloy catalysts. Common preparation methods include physical vapor deposition, chemical coprecipitation, sol-gel method, *etc.* Different preparation methods will affect the particle size, morphology, crystal structure, and surface properties of the alloy. The physical vapor deposition method can prepare alloy nanoparticles with uniform particle size and good dispersion^[181], which can increase the specific surface area of the catalyst and improve the exposure degree of active sites. The alloy catalyst prepared by the sol-gel method may have a more uniform element distribution and a better crystal structure, which is beneficial to improving the stability and activity of the catalyst.

Meanwhile, surface treatment of Rh-based alloy catalysts can further improve their performance. For example, methods such as surface oxidation and acid-washing (or acid leaching) can effectively remove impurities from the catalyst surface^[182,183], thereby restoring clean active sites and improving catalyst performance. In addition, by using the method of surface modification, such as loading some atoms or molecules with special functions on the alloy surface, the electronic and chemical properties of the alloy surface can also be regulated to optimize its catalytic performance for the HER. Table 5 presents the key performance parameters of recently reported Rh-based alloy HER catalysts used in acidic and alkaline environments.

Rh-based alloy catalysts achieve high activity, superior stability, and high atomic utilization through metal composition tuning, size and morphology optimization, crystal structure design, and interface coupling. Their performance enhancement mechanisms mainly include synergistic electronic effects, optimized surface active sites, interface synergy, and enhanced stability. Alloying provides an important strategy for designing efficient, durable, and resource-saving Rh-based HER catalysts.

Composites-type Rh-based catalysts

Rh-carbon-based composites are a common type of Rh-based catalyst, typically using carbon nanotubes, graphene, or activated carbon as supports. Carbon materials have advantages such as high specific surface area, good electrical conductivity, and chemical stability. Loading Rh nanoparticles on carbon-based materials can not only improve the dispersion of Rh and increase the number of active sites but also utilize the electrical conductivity of carbon materials to accelerate electron transfer, thereby increasing the reaction rate of the HER. For example, in the Rh-graphene composite^[134], the 2D structure of graphene provides a stable support for Rh nanoparticles. At the same time, the interaction between them can regulate the electronic structure of Rh and optimize the adsorption and desorption performance of hydrogen.

Rh-metal oxide composites are compounded with metal oxides such as Co_3O_4 , WO_3 , CoO , *etc.* Metal oxides have unique optical, electrical, and chemical properties, and a synergistic effect can be produced after being compounded with Rh. Zhang *et al.*^[203] successfully prepared a tungsten oxynitrides (WNO)-coupled Rh layer (Rh-WNO) for HER by simply heat-treating a urea sol-gel containing a mixed salt of tungsten and Rh. Rh nanoclusters are anchored on the surface of ordered WNO crystals through Rh-nitrogen and Rh-oxygen bonds. The optimal catalyst Rh-WNO requires low overpotentials of 19, 22, and 134 mV to achieve a current density of 10 mA cm^{-2} in 0.5 M H_2SO_4 , 1.0 M KOH, and 1.0 M PBS, respectively. Pan *et al.*^[204] introduced amorphous molybdenum oxide (MoO_x) at the atomic level into Rh hierarchical nanosheets (HNS) to prepare $\text{MoO}_x\text{Rh-HNS}$, which effectively reduced the barrier for hydrogen diffusion from Rh to MoO_x . Therefore, $\text{MoO}_x\text{Rh-HNS}$ exhibited excellent HER activity with a Tafel slope as low as 22.5 mV dec^{-1} ^[204]. DFT calculations showed that the adsorbed hydrogen on MoO_xRh promoted the dissociation of water and balanced the binding strength of hydrogen. Wu *et al.*^[205] also reported an efficient HER catalyst with atomically dispersed MoO_x species anchored on Rh metal. The morphology of the $\text{MoO}_x\text{-Rh}$ metallene

Table 5. Summary of the HER activity of Rh-based alloy used in acid and alkaline solutions

Catalyst	Activity (mV@mA cm ⁻²)		Stability	Ref.
	Acid	Alkaline		
RhNi	40@10 197@1000			[29]
e PtRhNiFeCu/C		13@10	20 h@10 mA cm ⁻²	[96]
d-HEA NPs	42.7@10		30 h@50 mA cm ⁻²	[89]
IrRuRhMoW/C	14@10	28@10	15 h@10 mA cm ⁻²	[47]
PdRhMoFeMn	6@10	26@10	20 h@10 mA cm ⁻²	[95]
HEA/GC	13@10	65@10	12 h@100 mV	[184]
RhRu _{0.5} -alloy wavy nanowire		54@100	80 h@100 mA cm ⁻²	[61]
Co AG-Rh500	13@10	17@10 84@100	20 h@100 mA cm ⁻²	[185]
Pt ₂₈ Mo ₆ Pd ₂₈ Rh ₂₇ Ni ₁₅ NCs		9.7@10 57.7@100	30 h@10 mA cm ⁻²	[186]
RhRuPtPdIr HEA thin film	58@10		20 h@10 mA cm ⁻²	[187]
PtPdRhRuCu MMNs	13@10	10@10	100 h@10, 20, 50, and 100 mA cm ⁻²	[176]
Rh ₃ Tb IMs		19@10	400 h@10 mA cm ⁻²	[179]
PtCoMoPdRh NFs		16.5@10	8 h@-0.05 V	[188]
NiRh _{0.016} -BDC		8@10	60 h@10 mA cm ⁻²	[30]
P-mAuRh film/NF		45@50	35 h@100 mA cm ⁻²	[189]
a-RhPb NFs		36@10	20 h@10 mA cm ⁻²	[190]
Au@Rh ₃ Cu	83@10			[191]
PtRh _{0.02} @Rh NWs		45.8@10	2,000 s@100 mA cm ⁻²	[192]
12-Fe@Cu-Rh	23@10	4@10	6 h@10 mA cm ⁻²	[193]
RhNi-2500	5.6@10	43.1@10	25 h@10 mA cm ⁻²	[31]
PtRuRhCoNi NWs/C	13@10		200 h@10 mA cm ⁻²	[175]
Rh _{2.6} Fe ₃ Co _{2.6} @NG		25@10	24 h@10 mA cm ⁻²	[194]
RhIr NSs/NF	14@10	15@10	20 h@10 mA cm ⁻²	[195]
Rh ₄₉ Ni ₅₁		59@10	10 h@10 mA cm ⁻²	[196]
Au@Rh@PEI MNs	30@10	29@10	24 h@10 mA cm ⁻²	[197]
PtPdRhIrNi NPNWs	22@10	55@10	24 h@10 mA cm ⁻²	[198]
Pt ₅₆ Rh ₄₄ NDs		20@10	10 h@10 mA cm ⁻²	[199]
PtRh DNAs	27@10	28@10	12 h@10 mA cm ⁻²	[200]
Au ₇₅ Rh ₂₅	64.1@10			[88]
RhCu NTs	12@10	8@10	12 h@10 mA cm ⁻²	[91]
RuRh ₂	34@10 44@50	24@10		[62]
Rh ³⁺ -NiFeCHH		36@50	12 h@50 mA cm ⁻²	[201]
Ni _x Rh _{1-x} @200 °C	24@10	37@10		[173]
PtRh NAA		55@10	24 h@30 mA cm ⁻²	[202]
Ni ₇ Rh ₃	48@10	107@10	25,000 s@10 mA cm ⁻²	[28]
PtRh-MoS ₂			1,200,000 s@20	[178]
RhCo-ANAs	31@10 (PBS)		180,00 s@-0.05 V	[177]

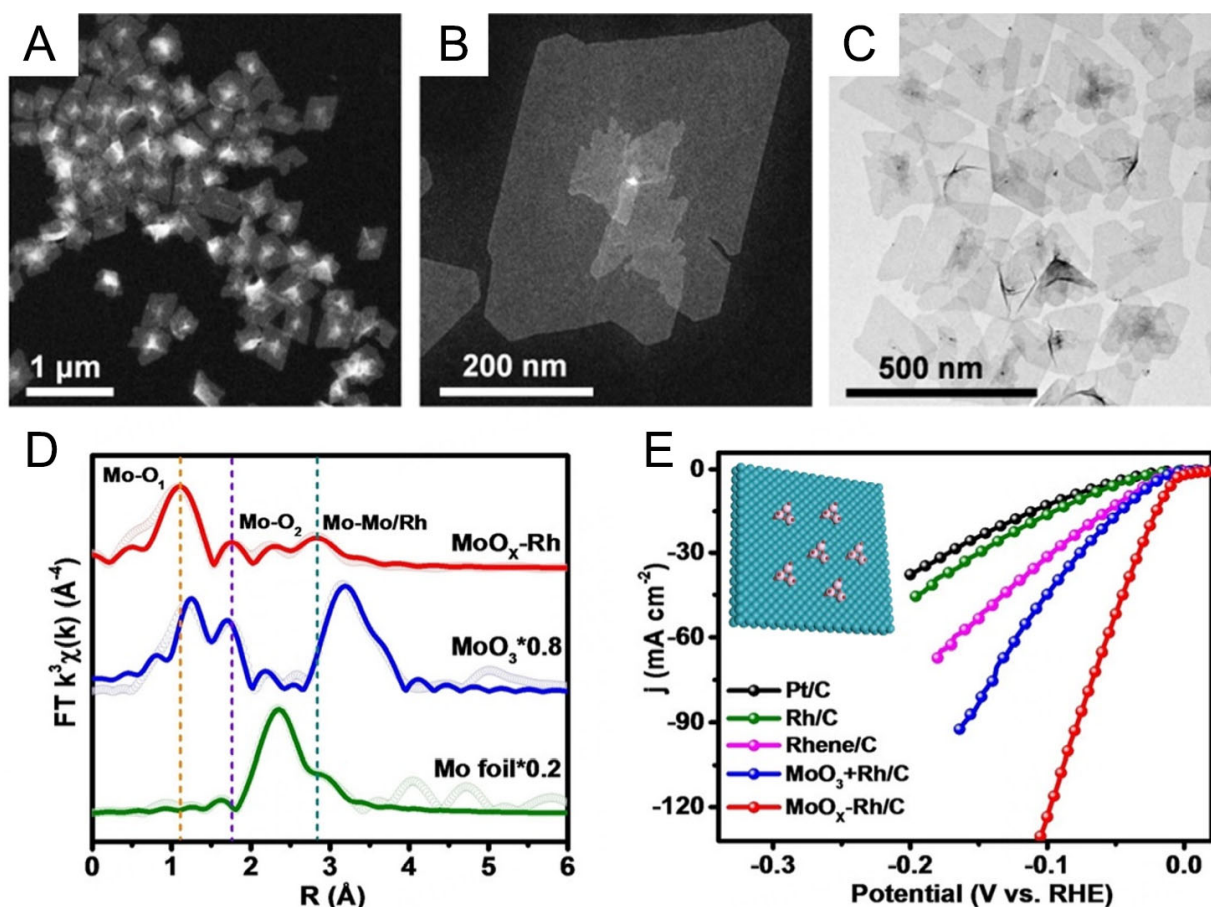


Figure 11. Morphological and structural characterizations of $\text{MoO}_x\text{-Rh}$ metallene: (A and B) HAADF-STEM and (C) TEM. (D) The k^3 -weighted $\chi(k)$ -function extracted from the EXAFS spectra is presented, where the dashed lines represent experimental data and the solid lines correspond to the fitted results. (E) HER polarization curves for commercial Pt/C, Rh/C, Rhene/C, $\text{MoO}_3 + \text{Rh/C}$, and $\text{MoO}_x\text{-Rh/C}$ catalysts. The inset provides a schematic illustration of the atomic structure of $\text{MoO}_x\text{-Rh}$ metallene, with Rh, molybdenum, and oxygen atoms represented by cyan, pink, and red spheres, respectively. This figure is reproduced from Ref.^[205] with permission. Copyright 2022, Wiley.

showed a graphene-like morphology with roughly flat surfaces [Figure 11A-C]. The obtained structure exposed the oxide-metal interface to the greatest extent. First-principles calculations demonstrated that the interface between MoO_x and Rh serves as the active site for hydrogen evolution in alkaline conditions. MoO_x sites exhibit a preference for facilitating the adsorption and dissociation of water molecules, while adjacent Rh sites are responsible for capturing the generated atomic hydrogen, thereby enhancing H_2 evolution efficiency [Figure 11D and E].

Meanwhile, according to different application scenarios and performance requirements, select appropriate support materials and conduct structural design and modification on them^[206,207]. For example, in situations where high electrical conductivity is required, graphene or carbon nanotubes and Ni cones can be selected as the support^[19,121,208-210], and surface treatment can be carried out on them to increase surface functional groups and improve the binding force with Rh.

Modify and functionalize the surface of Rh-based composites to regulate their surface properties and the interaction with reactants. Specific functional groups or molecules can be introduced on the surface of the composite through methods such as chemical adsorption, physical adsorption, or chemical reactions^[34,209]. For example, some co-catalysts such as sulfides and phosphides can also be loaded on the surface of the

Table 6. Summary of the HER activity of Rh-Based composite used in acid and alkaline solutions

Catalyst	Activity (mV@mA cm ⁻²)		Stability	Ref.
	Acid	Alkaline		
Rh-Rh ₂ O ₃		12@10		[211]
Rh ₂ O ₃ -NiWO ₄ /PNF		19@10 293@1,000	100 h@10 mA cm ⁻²	[212]
Pt/Rh ₂ O ₃ -CN _x		26.7@10	24 h@10 mA cm ⁻²	[42]
RhCrOx/FTO	175@10 (pH = 7)		-	[213]
MoOxRh-HNS		11.5@10 102.5@200	100 h@500 mA cm ⁻²	[204]
Rh-WNO	19@10	22@10	36,000 s@10 mA cm ⁻²	[203]
Rh-Co _x P		30@10	24 h@10 mA cm ⁻²	[214]
Rh-modified Co		270@10	-	[215]
Rh-WO ₃		98@10	60,000 s@10 mA cm ⁻²	[216]
Pt ₃ Rh-Co ₃ O ₄ /C	55@10		-	[217]
RhSn-MoS _x O _y	102@10			[218]
Nb ₂ RO ₄ /GDY		14@10	18 h@10 mA cm ⁻²	[219]
MoO _x -Rh		15@10	12 h@10 mA cm ⁻² 12 h@50 mA cm ⁻² 12 h@100 mA cm ⁻²	[205]
RhNi(OH) ₂ /C		36@10	3,200 s@10 mA cm ⁻²	[220]
Rh-modified Ni		110@10	60,000 s@10 mA cm ⁻²	[221]
Rh ₂ P/Rh-G	19@10	17@10		[222]
Rh-doped CoFe-ZLDH		28@10 188@10	10 h@10 mA cm ⁻²	[223]
Au ₆₈ Rh ₃₂ NFs		170@10	-	[224]
1D-Cu@Co-CoO/Rh		107.3@10 191.1@50		[225]
Fe,Rh-Ni ₂ P/NF		73@10	24 h@30 mA cm ⁻²	[209]

composite to further improve the hydrogen evolution performance. These co-catalysts can act synergistically with Rh, changing the intermediate steps and activation energy of the reaction, thus improving the catalytic activity. Table 6 presents the key performance parameters of recently reported Rh-based alloy composite catalysts used in acidic and alkaline environments.

Rh-based composite HER catalysts achieve a synergistic integration of high activity, superior stability, and high atomic utilization through composite support selection, multicomponent synergy, interface engineering, and nanostructure design. Their performance enhancement mainly arises from interface-induced electronic structure optimization, increased active site density, enhanced stability, and multifunctional synergistic effects. The composite strategy provides important design guidance for developing efficient, durable, and tunable Rh-based HER catalysts.

To visually demonstrate the activity and diversity of Rh-based HER catalysts in alkaline solutions, we will summarize representative Rh-based catalysts in Figure 12, including Rh composites, Rh alloys, Rh nanoparticles, Rh monoatomic, Rhenes, and Rh-based compounds. The comparison of their overpotentials clearly reveals the influence of composition and structure on the catalytic performance. Meanwhile, the corresponding performance under acidic solutions is summarized in Figure 13.

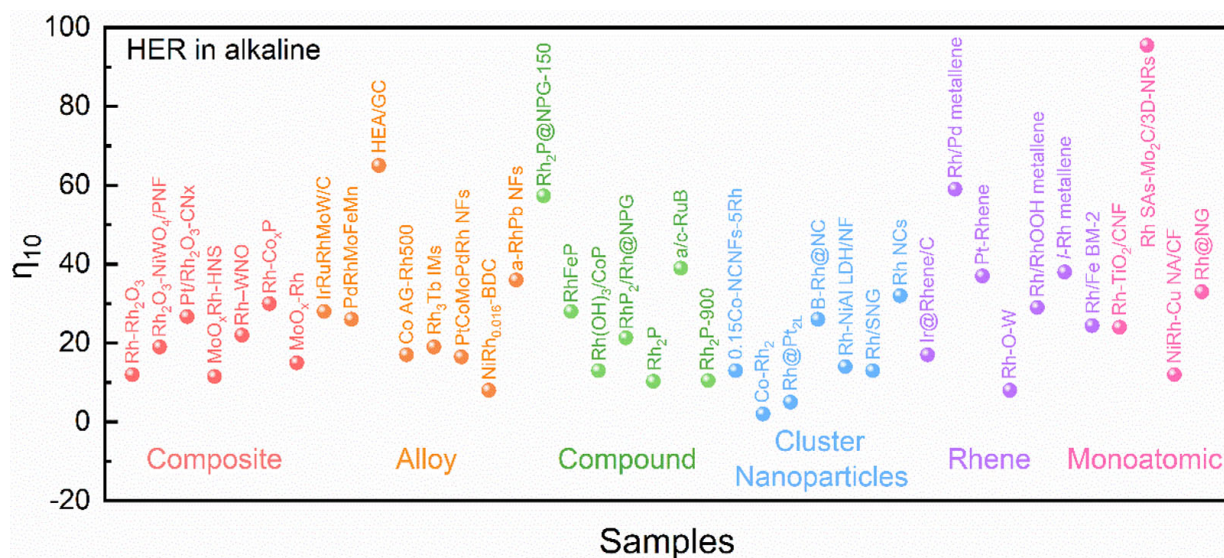


Figure 12. Summary of electrochemical activity of reported Rh-based catalysts in alkaline solutions.

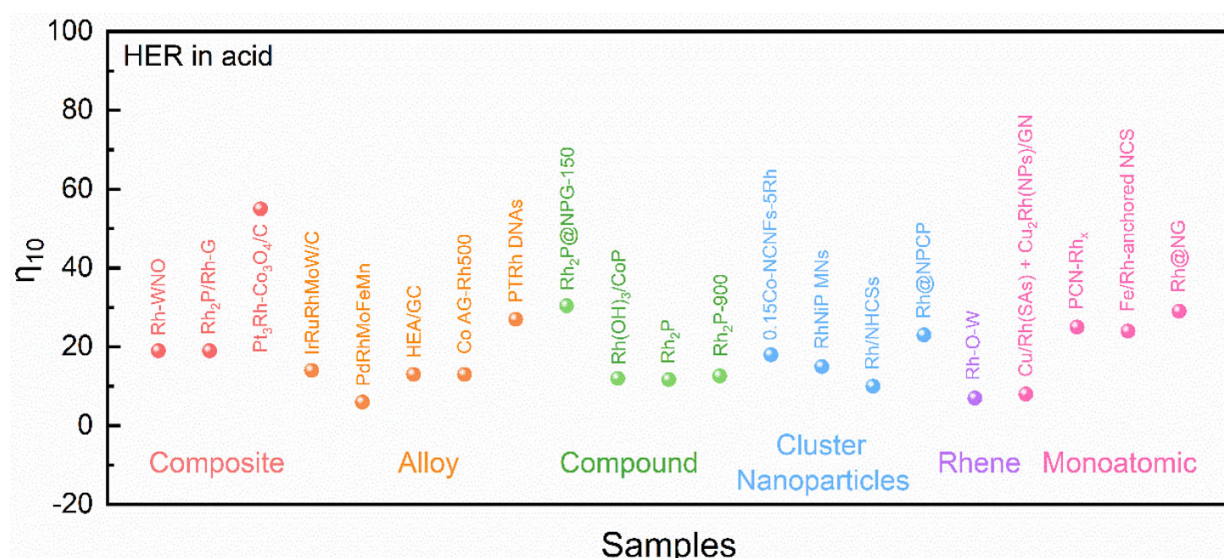


Figure 13. Summary of electrochemical activity of reported Rh-based catalysts in acidic solutions.

CONCLUSIONS AND PROSPECTS

Conclusions

Rh-based hydrogen evolution catalysts have demonstrated unique performance advantages and potential in recent research. Regarding the hydrogen evolution mechanism, aided by DFT calculations, we have clarified that under acidic and alkaline conditions, Rh-based catalysts effectively promote the elementary steps of the HER through their specific electronic structures, suitable hydrogen adsorption energies, and unique active sites. Under acidic conditions, precise regulation of hydrogen adsorption energy enables efficient coordination of the Volmer, Heyrovsky, and Tafel steps. In neutral conditions, effective catalysis of water adsorption and dissociation, along with optimization of subsequent hydrogen reaction pathways, ensures stable HER progress. In alkaline environments, excellent performance in lowering the water dissociation energy barrier and optimizing the hydrogen adsorption-desorption process distinguishes Rh-based catalysts. For the design of catalysts, computational simulations have developed some descriptors such as ΔG_{H^+} and

d-band center to describe their performance. Furthermore, machine learning algorithms have been introduced to accelerate the performance prediction and screening of catalysts.

Regarding catalyst types and optimization strategies, single-atom Rh-based catalysts exhibit high intrinsic activity due to their unique electronic structures, uniform active sites, and an almost 100% atomic utilization efficiency; heteroatom doping improves the catalytic performance by skillfully regulating the electronic structure, changing the crystal and surface properties, creating new active sites or optimizing the original ones. Rh-based catalysts supported on alkene materials achieve a dual improvement in activity and stability by virtue of the high specific surface area and good electrical conductivity of the alkene materials, as well as the electronic and confinement effects between them. For cluster and nanoparticle-type Rh-based catalysts, their size effects, crystal plane effects, and surface modification strategies provide multiple ways to optimize the catalytic performance. Rh-based compounds play a role in the HER through the characteristics of different compound types, such as the promotion of water dissociation by oxides and the regulation of the electronic structure by sulfides, and can be optimized through nanostructure design, composite doping, and surface modification. Rh-based alloys form alloys with different types of metals, changing the electronic and crystal structures, generating a synergistic effect, and improving the catalytic activity and stability. Their potential can be further explored through composition regulation, preparation method optimization, and surface treatment. Rh-based composites, such as those compounded with carbon-based materials, metal oxides, and organic polymers, take advantage of the strengths of each component. Through support selection and design, preparation process optimization, and surface modification and functionalization, they exhibit excellent hydrogen evolution performance.

Prospects

Although significant progress has been made in Rh-based hydrogen evolution catalysts, there is still broad room for development in the future. At the basic research level, it is necessary to further explore the structure-activity relationship of Rh-based catalysts under complex actual working conditions. Current research mostly focuses on ideal conditions, while there are various complex factors such as impurities, temperature fluctuations, and pressure changes in the actual water electrolysis system. A deep understanding of the influence of these factors on the catalyst performance will help to design and optimize the catalyst more accurately. Combining advanced *in-situ* characterization techniques, such as *in situ* X-ray diffraction, *in-situ* X-ray photoelectron spectroscopy and *in-situ* Raman spectroscopy^[226–228], to monitor the changes in the structure and electronic state of the catalyst in real time during the reaction process provides more direct experimental evidence for revealing the true reaction mechanism, further improves the DFT calculation model, and enhances the accuracy of theoretical predictions^[229].

In terms of material synthesis and preparation, the development of greener, more efficient, and lower-cost preparation technologies is crucial. Some current preparation methods have problems such as high energy consumption, complex processes, and the use of toxic and harmful reagents, which limit the large-scale application of Rh-based catalysts. Exploring new synthesis routes, such as using microbial synthesis and green chemical synthesis methods, can reduce the preparation cost and environmental impact while ensuring the performance of the catalyst^[230,231]. Meanwhile, precisely controlling the microstructure and composition of the catalyst to achieve atomic-level precise regulation can further enhance the performance and stability of the catalyst^[18,100].

From an application perspective, efforts should focus on accelerating the transition of Rh-based hydrogen evolution catalysts from laboratory research to industrial implementation. Close collaboration with relevant industries, the performance optimization and engineering design of the Rh-based catalysts should meet the needs of actual industrial water electrolysis devices^[232]. Developing Rh-based catalysts suitable for different

scales and types of water electrolysis equipment could improve their practicality and economic efficiency in large-scale production. In addition, we should expand the application of Rh-based catalysts in other related fields, such as photoelectrochemical hydrogen evolution and bioelectrocatalytic hydrogen evolution, even in other catalytic fields^[233]. Through interdisciplinary integration, integrating the knowledge and technologies of materials science, chemical engineering, electrochemistry, and computer simulations^[234,235], the innovative development of Rh-based hydrogen evolution catalysts could be extended to the entire hydrogen energy field.

DECLARATIONS

Authors' contributions

Substantial contributions to content discussion: Zhang, J.; Zhang, L.; Shen, S.; Qiu, C.; Wang J.

Draft manuscript preparation: Zhang, J.; Zhang L.

Assistance in draft preparation: Tian, L.; Zhang, H.; Jia, L.; Shi, X.

Manuscript revision before submission: Shen, S.; Zhong, W.; Qiu, C.; Wang, J.

Availability of data and materials

Not applicable.

Financial support and sponsorship

The authors acknowledge financial support from the National Natural Science Foundation of China (52472231, 52311530113, W2521017) and the Central Guidance on Science and Technology Development Fund of Zhejiang Province (2024ZY01011).

Conflicts of Interest

All authors declared that there are no conflicts of interest.

Ethical approval and consent to participate

Not applicable.

Consent for publication

Not applicable.

Copyright

© The Author(s) 2026.

REFERENCES

1. Mao, Q.; Wang, W.; Deng, K.; et al. Low-content Pt-triggered the optimized d-band center of Rh metallene for energy-saving hydrogen production coupled with hydrazine degradation. *J. Energy. Chem.* **2023**, *85*, 58-66. [DOI](#)
2. Zhu, L.; Lin, H.; Li, Y.; et al. A rhodium/silicon co-electrocatalyst design concept to surpass platinum hydrogen evolution activity at high overpotentials. *Nat. Commun.* **2016**, *7*, 12272. [DOI PubMed PMC](#)
3. Fan, J.; Cui, X.; Yu, S.; et al. Interstitial hydrogen atom modulation to boost hydrogen evolution in Pd-based alloy nanoparticles. *ACS. Nano.* **2019**, *13*, 12987-95. [DOI PubMed](#)
4. Yan, Z.; Gong, J.; Sun, H.; et al. Heterojunction-doping synergy in strontium palladium-ruthenium oxide catalysts for efficient oxygen evolution. *Nano. Res.* **2025**. [DOI](#)
5. Prabhu, P.; Do, V. H.; Peng, C. K.; et al. Oxygen-bridged stabilization of single atomic W on Rh metallenes for robust and efficient pH-universal hydrogen evolution. *ACS. Nano.* **2023**, *17*, 10733-47. [DOI PubMed](#)
6. Zheng, Y.; Zhang, B.; Ma, T.; et al. Nitrided rhodium nanoclusters with optimized water bonding and splitting effects for pH-universal H₂-production. *Small* **2023**, *20*, 2307405. [DOI PubMed](#)
7. Xing, M.; Zhu, S.; Zeng, X.; Wang, S.; Liu, Z.; Cao, D. Amorphous/Crystalline Rh(OH)₃/CoP heterostructure with hydrophilicity/aerophobicity feature for all-pH hydrogen evolution reactions. *Adv. Energy. Mater.* **2023**, *13*, 2302376. [DOI](#)
8. Xu, X.; Zhong, Y.; Wajrak, M.; Bhatelia, T.; Jiang, S. P.; Shao, Z. Grain boundary engineering: an emerging pathway toward efficient electrocatalysis. *InfoMat* **2024**, *6*, e12608. [DOI](#)

9. Jamadar, A. S.; Sutar, R.; Patil, S.; Khandekar, R.; Yadav, J. B. Progress in metal oxide-based electrocatalysts for sustainable water splitting. *Mater. Rep. Energy*. **2024**, *4*, 100283. DOI
10. Zhang, X.; Song, J.; Sun, T.; et al. Constructing nanoneedle arrays of heterostructured $\text{RuO}_2\text{-Co}_3\text{O}_4$ with tip-effect-induced enrichment of reactants for enhanced water oxidation. *Chem. Commun.* **2025**, *61*, 8723-6. DOI PubMed
11. Wang, Y.; Guo, W.; Zhu, Z.; et al. Interfacial boron modification on mesoporous octahedral rhodium shell and its enhanced electrocatalysis for water splitting and oxygen reduction. *Chem. Eng. J.* **2022**, *435*, 134982. DOI
12. Guo, Y.; Yang, X.; Liu, X.; Tong, X.; Yang, N. Coupling methanol oxidation with hydrogen evolution on bifunctional co-doped Rh electrocatalyst for efficient hydrogen generation. *Adv. Funct. Mater.* **2022**, *33*, 2209134. DOI
13. Guo, Y.; Hou, B.; Cui, X.; Liu, X.; Tong, X.; Yang, N. Pt atomic layers boosted hydrogen evolution reaction in nonacidic media. *Adv. Energy Mater.* **2022**, *12*, 2201548. DOI
14. Wang, K.; Huang, B.; Lin, F.; et al. Wrinkled Rh_2P nanosheets as superior pH-universal electrocatalysts for hydrogen evolution catalysis. *Adv. Energy Mater.* **2018**, *8*, 1801891. DOI
15. Jiang, Y.; Leng, J.; Zhang, S.; et al. Modulating water splitting kinetics via charge transfer and interfacial hydrogen spillover effect for robust hydrogen evolution catalysis in alkaline media. *Adv. Sci.* **2023**, *10*, e2302358. DOI PubMed PMC
16. Li, Q.; Zhang, H.; Yang, D.; et al. Cationic defect-enabled charge transfer in rhodium clusters via Rh-O bonding for enhanced alkaline hydrogen evolution. *Nano. Res.* **2025**, *18*, 94907391. DOI
17. Ding, R.; Yan, T.; Wang, Y.; Long, Y.; Fan, G. Carbon nanopore and anchoring site-assisted general construction of encapsulated metal (Rh, Ru, Ir) nanoclusters for highly efficient hydrogen evolution in pH-universal electrolytes and natural seawater. *Green. Chem.* **2021**, *23*, 4551-9. DOI
18. Li, F.; Yao, C.; Jeon, J. P.; et al. Rhodium and carbon sites with strong d-p orbital interaction for efficient bifunctional catalysis. *ACS. Nano.* **2023**, *17*, 24282-9. DOI PubMed
19. Tareq, F. K.; Lee, H.; Shin, C.; Kojo, S. I.; Yu, J. Honeycomb-structured S and N-codoped highly graphitized carbon as a catalyst support for Rh nanoparticles: a new benchmark electrocatalyst for hydrogen evolution reaction. *Electrochim. Acta.* **2024**, *498*, 144627. DOI
20. Liu, T.; Chen, C.; Pu, Z.; et al. Joule heating to grain-boundary-rich RuP_2 for efficient electrocatalytic hydrogen evolution in a wide pH range. *Energy Mater.* **2025**, *5*, 500058. DOI
21. Obiang Nsang, G. E.; Ullah, B.; Hua, S.; et al. NiS nanoparticle- MoS_2 nanosheet core-shell spheres: PVP-assisted synthesis and efficient electrocatalyst for hydrogen evolution reaction. *Energy Mater.* **2025**, *5*, 500047. DOI
22. Liu, D.; Xu, G.; Yang, H.; Wang, H.; Xia, B. Y. Rational design of transition metal phosphide-based electrocatalysts for hydrogen evolution. *Adv. Funct. Mater.* **2022**, *33*, 2208358. DOI
23. Wang, H.; Ren, J.; Wang, L.; et al. Synergistically enhanced activity and stability of bifunctional nickel phosphide/sulfide heterointerface electrodes for direct alkaline seawater electrolysis. *J. Energy. Chem.* **2022**, *75*, 66-73. DOI
24. Lu, Y.; Yue, C.; Li, Y.; et al. Atomically dispersed Ni on Mo_2C embedded in N, P co-doped carbon derived from polyoxometalate supramolecule for high-efficiency hydrogen evolution electrocatalysis. *Appl. Catal. B. Environ.* **2021**, *296*, 120336. DOI
25. Cao, Y. Roadmap and direction toward high-performance MoS_2 hydrogen evolution catalysts. *ACS. Nano.* **2021**, *15*, 11014-39. DOI PubMed
26. Vij, V.; Sultan, S.; Harzandi, A. M.; et al. Nickel-based electrocatalysts for energy-related applications: oxygen reduction, oxygen evolution, and hydrogen evolution reactions. *ACS. Catal.* **2017**, *7*, 7196-225. DOI
27. Cheng, Y.; Lu, S.; Liao, F.; Liu, L.; Li, Y.; Shao, M. Rh - MoS_2 nanocomposite catalysts with Pt-like activity for hydrogen evolution reaction. *Adv. Funct. Mater.* **2017**, *27*, 1700359. DOI
28. Nguyen, N.; Nguyen, V.; Shin, S.; Choi, H. NiRh nanosponges with highly efficient electrocatalytic performance for hydrogen evolution reaction. *J. Alloys. Compd.* **2019**, *789*, 163-73. DOI
29. Ehsan, M. A.; Aftab, F.; Younas, M.; Mansoor, M. A.; Ahmed, S. Graphite sheet-supported bimetallic RhNi thin film alloys for enhanced and durable hydrogen evolution in acidic environments. *Int. J. Hydrogen. Energy.* **2024**, *69*, 411-20. DOI
30. Xu, X.; Chen, H. C.; Li, L.; et al. Leveraging metal nodes in metal-organic frameworks for advanced anodic hydrazine oxidation assisted seawater splitting. *ACS. Nano.* **2023**, *17*, 10906-17. DOI PubMed
31. Zhai, Z.; Wang, Y.; Si, C.; et al. Self-templating synthesis and structural regulation of nanoporous rhodium-nickel alloy nanowires efficiently catalyzing hydrogen evolution reaction in both acidic and alkaline electrolytes. *Nano Res.* **2022**, *16*, 2026-34. DOI
32. Yu, Q.; Fu, Y.; Zhao, J.; et al. Boron doping activate strong metal-support interaction for electrocatalytic hydrogen evolution reaction in full pH range. *Appl. Catal. B. Environ.* **2023**, *324*, 122297. DOI
33. Lin, G.; Zhang, Z.; Ju, Q.; et al. Bottom-up evolution of perovskite clusters into high-activity rhodium nanoparticles toward alkaline hydrogen evolution. *Nat. Commun.* **2023**, *14*, 280. DOI PubMed PMC

-
34. Chen, X.; Li, W.; Wang, C.; Lu, X. Wet chemical synthesis of rhodium nanoparticles anchored on cobalt/nitrogen-doped carbon nanofibers for high-performance alkaline and acidic hydrogen evolution. *J. Colloid. Interface. Sci.* **2023**, *650*, 304–12. [DOI PubMed](#)
35. Wang, Q.; Ming, M.; Niu, S.; Zhang, Y.; Fan, G.; Hu, J. S. Scalable solid-state synthesis of highly dispersed uncapped metal (Rh, Ru, Ir) nanoparticles for efficient hydrogen evolution. *Adv. Energy. Mater.* **2018**, *8*, 1801698. [DOI](#)
36. Zhao, Y.; Xing, S.; Meng, X.; et al. Ultrathin Rh nanosheets as a highly efficient bifunctional electrocatalyst for isopropanol-assisted overall water splitting. *Nanoscale* **2019**, *11*, 9319–26. [DOI PubMed](#)
37. Gao, Y.; Xue, Y.; Qi, L.; et al. Rhodium nanocrystals on porous graphdiyne for electrocatalytic hydrogen evolution from saline water. *Nat. Commun.* **2022**, *13*, 5227. [DOI PubMed PMC](#)
38. Ming, M.; Zhang, Y.; He, C.; et al. Room-temperature sustainable synthesis of selected platinum group metal (PGM = Ir, Rh, and Ru) nanocatalysts well-dispersed on porous carbon for efficient hydrogen evolution and oxidation. *Small* **2019**, *15*, e1903057. [DOI PubMed](#)
39. Liu, Y.; Hu, X.; Huang, B.; Xie, Z. Surface engineering of Rh catalysts with N/S-codoped carbon nanosheets toward high-performance hydrogen evolution from seawater. *ACS. Sustain. Chem. Eng.* **2019**, *7*, 18835–43. [DOI](#)
40. Logeshwaran, N.; Kim, G.; Thangavel, P.; et al. Synergistic configuration of binary rhodium single atoms in carbon nanofibers for high-performance alkaline water electrolyzer. *Adv. Sci.* **2025**, *12*, e2413176. [DOI PubMed PMC](#)
41. Wang, W.; Geng, W.; Zhang, L.; et al. Molybdenum oxycarbide supported Rh-clusters with modulated interstitial C-O microenvironments for promoting hydrogen evolution. *Small* **2023**, *19*, e2206808. [DOI PubMed](#)
42. Kumar Manna, B.; Samanta, R.; Kumar Trivedi, R.; Chakraborty, B.; Barman, S. Hydrogen spillover inspired bifunctional platinum/rhodium oxide-nitrogen-doped carbon composite for enhanced hydrogen evolution and oxidation reactions in base. *J. Colloid. Interface. Sci.* **2024**, *670*, 258–71. [DOI PubMed](#)
43. Sun, B.; Zhong, W.; Liu, H.; Ai, X.; Han, S.; Chen, Y. Controlling rhodium-based nanomaterials for high-efficiency energy-related electrocatalysis. *EnergyChem* **2025**, *7*, 100148. [DOI](#)
44. Li, Y.; Liu, X.; Xu, J.; Chen, S. Ruthenium-based electrocatalysts for hydrogen evolution reaction: from nanoparticles to single atoms. *Small* **2024**, *20*, e2402846. [DOI PubMed](#)
45. Jia, N.; Liu, Y.; Wang, L.; et al. 0.2 V electrolysis voltage-driven alkaline hydrogen production with nitrogen-doped carbon nanobowl-supported ultrafine Rh nanoparticles of 1.4 nm. *ACS. Appl. Mater. Interfaces.* **2019**, *11*, 35039–49. [DOI PubMed](#)
46. Wang, C.; Zhang, Q.; Yan, B.; et al. Facet engineering of advanced electrocatalysts toward hydrogen/oxygen evolution reactions. *Nanomicro. Lett.* **2023**, *15*, 52. [DOI PubMed PMC](#)
47. Luo, H.; Li, L.; Lin, F.; et al. Sub-2 nm microstrained high-entropy-alloy nanoparticles boost hydrogen electrocatalysis. *Adv. Mater.* **2024**, *36*, e2403674. [DOI PubMed](#)
48. Guo, F.; Macdonald, T. J.; Sobrido, A. J.; Liu, L.; Feng, J.; He, G. Recent advances in ultralow-Pt-loading electrocatalysts for the efficient hydrogen evolution. *Adv. Sci.* **2023**, *10*, e2301098. [DOI PubMed PMC](#)
49. Zhai, W.; Ma, Y.; Chen, D.; Ho, J. C.; Dai, Z.; Qu, Y. Recent progress on the long-term stability of hydrogen evolution reaction electrocatalysts. *InfoMat* **2022**, *4*, e12357. [DOI](#)
50. Zhou, X.; Hensen, E. J.; van Santen, R. A.; Li, C. DFT simulations of water adsorption and activation on low-index α -Ga₂O₃ surfaces. *Chemistry* **2014**, *20*, 6915–26. [DOI PubMed](#)
51. Dubouis, N.; Grimaud, A. The hydrogen evolution reaction: from material to interfacial descriptors. *Chem. Sci.* **2019**, *10*, 9165–81. [DOI PubMed PMC](#)
52. Jung, O.; Jackson, M. N.; Bisbey, R. P.; Kogan, N. E.; Surendranath, Y. Innocent buffers reveal the intrinsic pH- and coverage-dependent kinetics of the hydrogen evolution reaction on noble metals. *Joule* **2022**, *6*, 476–93. [DOI](#)
53. Zheng, X.; Shi, X.; Ning, H.; et al. Tailoring a local acid-like microenvironment for efficient neutral hydrogen evolution. *Nat. Commun.* **2023**, *14*, 4209. [DOI PubMed PMC](#)
54. Andrew, A. A.; Abild-Pedersen, F.; Studt, F.; Rossmeisl, J.; Nørskov, J. K. How copper catalyzes the electroreduction of carbon dioxide into hydrocarbon fuels. *Energy. Environ. Sci.* **2010**, *3*, 1311–15. [DOI](#)
55. Bhunia, K.; Chandra, M.; Kumar Sharma, S.; Pradhan, D.; Kim, S. A critical review on transition metal phosphide based catalyst for electrochemical hydrogen evolution reaction: Gibbs free energy, composition, stability, and true identity of active site. *Coord. Chem. Rev.* **2023**, *478*, 214956. [DOI](#)
56. Nørskov, J. K.; Bligaard, T.; Logadottir, A.; et al. Trends in the exchange current for hydrogen evolution. *J. Electrochem. Soc.* **2005**, *152*, J23. [DOI](#)
57. Megha; Sen, P. From the single-atom limit to the mixed-metal phase: finding the optimum condition for activating the basal plane of a FePSe₃ monolayer towards HER. *Phys. Chem. Chem. Phys.* **2023**, *25*, 17269–80. [DOI PubMed](#)
58. Zhou, Y.; Song, E.; Chen, W.; et al. Dual-metal interbonding as the chemical facilitator for single-atom dispersions. *Adv. Mater.* **2020**, *32*, e2003484. [DOI PubMed](#)

-
59. Sultan, S.; Diorizky, M. H.; Ha, M.; et al. Modulation of Cu and Rh single-atoms and nanoparticles for high-performance hydrogen evolution activity in acidic media. *J. Mater. Chem. A*. **2021**, *9*, 10326–34. [DOI](#)
60. Nguyen, D. C.; Doan, T. L. L.; Prabhakaran, S.; Kim, D. H.; Kim, N. H.; Lee, J. H. Rh single atoms/clusters confined in metal sulfide/oxide nanotubes as advanced multifunctional catalysts for green and energy-saving hydrogen productions. *Appl. Catal. B. Environ.* **2022**, *313*, 121430. [DOI](#)
61. Fu, X.; Cheng, D.; Wan, C.; et al. Bifunctional ultrathin RhRu_{0.5}-alloy nanowire electrocatalysts for hydrazine-assisted water splitting. *Adv. Mater.* **2023**, *35*, e2301533. [DOI PubMed](#)
62. Mu, X.; Gu, J.; Feng, F.; et al. RuRh bimetallic nanoring as high-efficiency pH-universal catalyst for hydrogen evolution reaction. *Adv. Sci.* **2021**, *8*, 2002341. [DOI PubMed PMC](#)
63. Sun, F.; Tang, Q.; Jiang, D. Theoretical advances in understanding and designing the active sites for hydrogen evolution reaction. *ACS Catal.* **2022**, *12*, 8404–33. [DOI](#)
64. Abd Elhamid, M. H.; Ateya, B. G.; Weil, K. G.; Pickering, H. W. Calculation of the hydrogen surface coverage and rate constants of the hydrogen evolution reaction from polarization data. *J. Electrochem. Soc.* **2000**, *147*, 2148. [DOI](#)
65. Shi, Y.; Zhou, Y.; Yang, D. R.; et al. Energy level engineering of MoS₂ by transition-metal doping for accelerating hydrogen evolution reaction. *J. Am. Chem. Soc.* **2017**, *139*, 15479–85. [DOI](#)
66. Zhang, L.; Wang, Z.; Zhang, J.; et al. High activity and stability in Ni₂P/(Co,Ni)OOH heterointerface with a multiple-hierarchy structure for alkaline hydrogen evolution reaction. *Nano. Res.* **2023**, *16*, 6552–9. [DOI](#)
67. Yan, Z.; Liu, Z.; Zhou, G.; et al. Short-path hydrogen spillover on CeO₂-supported PtPd nanoclusters for efficient hydrogen evolution in acidic media. *Angew. Chem. Int. Ed.* **2025**, *64*, e202501964. [DOI PubMed](#)
68. Zhang, L.; Shi, X.; Xu, A.; Zhong, W.; Zhang, J.; Shen, S. Novel CoP/CoMoP₂ heterojunction with nanoporous structure as an efficient electrocatalyst for hydrogen evolution. *Nano. Res.* **2023**, *17*, 3693–9. [DOI](#)
69. Lu, J.; Hou, X.; Xiao, B.; Xu, X.; Mi, J.; Zhang, P. Computational screening of transition-metal doped boron nanotubes as efficient electrocatalysts for water splitting. *RSC Adv.* **2022**, *12*, 6841–7. [DOI PubMed PMC](#)
70. Fang, C.; Liu, D.; Zhang, Q.; Liu, G.; Shi, C.; Xu, J. In pursuit of a bifunctional designing toward highly efficient overall water splitting in a hydrogen-functionalized two-dimensional covalent organic framework via single transition metal mapping. *Int. J. Hydrogen. Energy*. **2024**, *62*, 48–61. [DOI](#)
71. Hammer, B.; Nørskov, J. Electronic factors determining the reactivity of metal surfaces. *Surf. Sci.* **1995**, *343*, 211–20. [DOI](#)
72. Shen, S.; Wang, Z.; Lin, Z.; et al. Crystalline-amorphous interfaces coupling of CoSe₂/CoP with optimized d-band center and boosted electrocatalytic hydrogen evolution. *Adv. Mater.* **2022**, *34*, e2110631. [DOI PubMed](#)
73. Doan, T. L. L.; Nguyen, D. C.; Bacirhonde, P. M.; et al. Atomic dispersion of Rh on interconnected Mo₂C nanosheet network intimately embedded in 3D Ni_xMoO₄ nanorod arrays for pH-universal hydrogen evolution. *Energy. Environ. Mater.* **2023**, *6*, e12407. [DOI](#)
74. Kundu, M. K.; Mishra, R.; Bhowmik, T.; Barman, S. Rhodium metal-rhodium oxide (Rh-Rh₂O₃) nanostructures with Pt-like or better activity towards hydrogen evolution and oxidation reactions (HER, HOR) in acid and base: correlating its HOR/HER activity with hydrogen binding energy and oxophilicity of the catalyst. *J. Mater. Chem. A*. **2018**, *6*, 23531–41. [DOI](#)
75. Chen, K.; Wang, Z.; Wang, L.; et al. Boron nanosheet-supported Rh catalysts for hydrogen evolution: a new territory for the strong metal-support interaction effect. *Nanomicro. Lett.* **2021**, *13*, 138. [DOI PubMed PMC](#)
76. Mao, Q.; Deng, K.; Yu, H.; et al. In situ reconstruction of partially hydroxylated porous Rh metallene for ethylene glycol-assisted seawater splitting. *Adv. Funct. Mater.* **2022**, *32*, 2201081. [DOI](#)
77. An, Q.; Bo, S.; Jiang, J.; et al. Atomic-level interface engineering for boosting oxygen electrocatalysis performance of single-atom catalysts: from metal active center to the first coordination sphere. *Adv. Sci.* **2023**, *10*, e2205031. [DOI PubMed PMC](#)
78. Guo, W.; Dun, C.; Yu, C.; et al. Mismatching integration-enabled strains and defects engineering in LDH microstructure for high-rate and long-life charge storage. *Nat. Commun.* **2022**, *13*, 1409. [DOI PubMed PMC](#)
79. Zhu, Y. P.; Guo, C.; Zheng, Y.; Qiao, S. Z. Surface and interface engineering of noble-metal-free electrocatalysts for efficient energy conversion processes. *Acc. Chem. Res.* **2017**, *50*, 915–23. [DOI PubMed](#)
80. Calle-Vallejo, F.; Bandarenka, A. S. Enabling generalized coordination numbers to describe strain effects. *ChemSusChem* **2018**, *11*, 1824–8. [DOI PubMed](#)
81. Du, J.; Yan, Y.; Li, X.; et al. A mechanism-guided descriptor for the hydrogen evolution reaction in 2D ordered double transition-metal carbide MXenes. *Chem. Sci.* **2025**, *16*, 9424–35. [DOI](#)
82. Calle-Vallejo, F. The ABC of generalized coordination numbers and their use as a descriptor in electrocatalysis. *Adv. Sci.* **2023**, *10*, e2207644. [DOI PubMed PMC](#)
83. Ding, R.; Chen, J.; Chen, Y.; Liu, J.; Bando, Y.; Wang, X. Unlocking the potential: machine learning applications in electrocatalyst design for electrochemical hydrogen energy transformation. *Chem. Soc. Rev.* **2024**, *53*, 11390–461. [DOI PubMed](#)

-
84. Lu, Z.; Yadav, S.; Singh, C. V. Predicting aggregation energy for single atom bimetallic catalysts on clean and O* adsorbed surfaces through machine learning models. *Catal. Sci. Technol.* **2020**, *10*, 86–98. DOI
85. Xu, P.; Ji, X.; Li, M.; Lu, W. Small data machine learning in materials science. *NPJ. Comput. Mater.* **2023**, *9*, 42. DOI
86. Hoffmann, N.; Schmidt, J.; Botti, S.; Marques, M. A. L. Transfer learning on large datasets for the accurate prediction of material properties. *Digital. Discovery*. **2023**, *2*, 1368–79. DOI
87. Cai, J.; Liao, X.; Li, P.; et al. Penta-twinned Rh@Pt core-shell nanobranches with engineered shell thickness for reversible and active hydrogen redox electrocatalysis. *Chem. Eng. J.* **2022**, *429*, 132414. DOI
88. Bian, T.; Xiao, B.; Sun, B.; et al. Local epitaxial growth of Au-Rh core-shell star-shaped decahedra: a case for studying electronic and ensemble effects in hydrogen evolution reaction. *Appl. Catal. B. Environ.* **2020**, *263*, 118255. DOI
89. Huang, X.; Wu, Z.; Zhang, B.; et al. Formation of disordered high-entropy-alloy nanoparticles for highly efficient hydrogen electrocatalysis. *Small* **2024**, *20*, e2311631. DOI PubMed
90. Golubović, J.; Rakočević, L.; Latas, N.; Varničić, M.; Rajić, V.; Štrbac, S. Enhanced hydrogen evolution catalysis on Rh nanoparticles with low loading on graphene nanoplatelets. *Appl. Surf. Sci.* **2024**, *672*, 160805. DOI
91. Cao, D.; Xu, H.; Cheng, D. Construction of defect-rich RhCu nanotubes with highly active Rh₃Cu₁ alloy phase for overall water splitting in all pH values. *Adv. Energy. Mater.* **2020**, *10*, 1903038. DOI
92. Volpato, G. A.; Muneton Arboleda, D.; Brandiele, R.; et al. Clean rhodium nanoparticles prepared by laser ablation in liquid for high performance electrocatalysis of the hydrogen evolution reaction. *Nanoscale. Adv.* **2019**, *1*, 4296–300. DOI PubMed PMC
93. Fu, X.; Zhao, Z.; Wan, C.; et al. Ultrathin wavy Rh nanowires as highly effective electrocatalysts for methanol oxidation reaction with ultrahigh ECSA. *Nano. Res.* **2018**, *12*, 211–5. DOI
94. Zheng, L.; Xu, L.; Gu, P.; Chen, Y. Lattice engineering of noble metal-based nanomaterials via metal-nonmetal interactions for catalytic applications. *Nanoscale* **2024**, *16*, 7841–61. DOI PubMed
95. Li, Y.; Peng, C. K.; Sun, Y.; et al. Operando elucidation of hydrogen production mechanisms on sub-nanometric high-entropy metallenes. *Nat. Commun.* **2024**, *15*, 10222. DOI PubMed PMC
96. Hu, Z.; Chen, K.; Zhu, Y.; Liu, B.; Shen, J. Synergistic effects of PtRhNiFeCu high entropy alloy nanocatalyst for hydrogen evolution and oxygen reduction reactions. *Small* **2024**, *20*, e2309819. DOI PubMed
97. Li, X.; Huang, Y.; Chen, Z.; et al. Novel PtNi nanoflowers regulated by a third element (Rh, Ru, Pd) as efficient multifunctional electrocatalysts for ORR, MOR and HER. *Chem. Eng. J.* **2023**, *454*, 140131. DOI
98. Jiang, B.; Huang, A.; Wang, T.; et al. Rhodium/graphitic-carbon-nitride composite electrocatalyst facilitates efficient hydrogen evolution in acidic and alkaline electrolytes. *J. Colloid. Interface. Sci.* **2020**, *571*, 30–7. DOI PubMed
99. Jia, M.; Jiang, G.; Chen, H.; et al. Recent developments on processes for recovery of rhodium metal from spent catalysts. *Catalysts* **2022**, *12*, 1415. DOI
100. Dong, H.; Zhao, Z.; Wu, Z.; et al. Metal-oxo cluster mediated atomic Rh with high accessibility for efficient hydrogen evolution. *Small* **2023**, *19*, e2207527. DOI PubMed
101. Yan, K.; Wei, T.; Ren, H.; et al. Asymmetric exchange interaction induces highly efficient alkaline hydrogen evolution in RhFe bimetallic. *Small* **2022**, *18*, e2204456. DOI PubMed
102. Zhang, B.; Zhu, C.; Wu, Z.; et al. Integrating Rh species with NiFe-layered double hydroxide for overall water splitting. *Nano. Lett.* **2020**, *20*, 136–44. DOI
103. Liu, Y.; Ding, J.; Li, F.; et al. Modulating hydrogen adsorption via charge transfer at the semiconductor-metal heterointerface for highly efficient hydrogen evolution catalysis. *Adv. Mater.* **2023**, *35*, e2207114. DOI PubMed
104. Tran, N. Q.; Le, B. T. N.; Le, T. N.; et al. Coupling amorphous Ni hydroxide nanoparticles with single-atom Rh on Cu nanowire arrays for highly efficient alkaline seawater electrolysis. *J. Phys. Chem. Lett.* **2022**, *13*, 8192–9. DOI PubMed
105. Guan, J.; Wen, X.; Zhang, Q.; Duan, Z. Atomic rhodium catalysts for hydrogen evolution and oxygen reduction reactions. *Carbon* **2020**, *164*, 121–8. DOI
106. Cao, C.; Xu, Q.; Zhu, Q. L. Ultrathin two-dimensional metallenes for heterogeneous catalysis. *Chem. Catal.* **2022**, *2*, 693–723. DOI
107. Xie, M.; Tang, S.; Zhang, B.; Yu, G. Metallene-related materials for electrocatalysis and energy conversion. *Mater. Horiz.* **2023**, *10*, 407–31. DOI PubMed
108. Wang, Z.; Yang, G.; Tian, P.; et al. Heterointerface engineering of Rh/Pd metallene for hydrazine oxidation-assisted energy-saving hydrogen production. *J. Mater. Chem. A.* **2023**, *11*, 10222–7. DOI
109. Deng, K.; Mao, Q.; Wang, W.; et al. Defect-rich low-crystalline Rh metallene for efficient chlorine-free H₂ production by hydrazine-assisted seawater splitting. *Appl. Catal. B. Environ.* **2022**, *310*, 121338. DOI
110. Piotrowski, M. J.; Piquini, P.; Cândido, L.; Da Silva, J. L. The role of electron localization in the atomic structure of transition-metal 13-atom clusters: the example of Co₁₃, Rh₁₃, and Hf₁₃. *Phys. Chem. Chem. Phys.* **2011**, *13*, 17242–8. DOI PubMed

-
111. Luo, G.; Song, M.; Zhang, Q.; et al. Advances of synergistic electrocatalysis between single atoms and nanoparticles/clusters. *Nano-Micro. Lett.* **2024**, *16*, 241. DOI PubMed PMC
112. Lin, S.; Li, D.; Zhang, D.; et al. Privileged metal cluster complexes. *Chem. Sci.* **2025**, *16*, 11619-25. DOI PubMed PMC
113. Guo, Y.; Wang, Y.; Huang, Z.; Tong, X.; Yang, N. Size effect of Rhodium nanoparticles supported on carbon black on the performance of hydrogen evolution reaction. *Carbon* **2022**, *194*, 303-9. DOI
114. Cao, K. W.; Sun, H. Y.; Xue, Q.; et al. Functionalized ultrafine rhodium nanoparticles on graphene aerogels for the hydrogen evolution reaction. *ChemElectroChem* **2021**, *8*, 1759-65. DOI
115. Zhang, Y.; Grass, M. E.; Habas, S. E.; et al. One-step polyol synthesis and langmuir-blodgett monolayer formation of size-tunable monodisperse rhodium nanocrystals with catalytically active (111) surface structures. *J. Phys. Chem. C* **2007**, *111*, 12243-53. DOI
116. Sookhakian, M.; Siburian, R.; Tong, G. B.; Mat Teridi, M. A.; Mahmoud, E.; Alias, Y. Ratio design of bimetallic Pd-Rh nanoparticles on MoS₂ nanosheets: excellent electrocatalysts for hydrogen evolution reaction. *Appl. Organomet. Chem.* **2024**, *38*, e7541. DOI
117. Bonifacio, R. M.; Mena, M. G. Activity of electrodeposited rhodium in acidic and basic water electrolysis. *Int. J. Hydrogen. Energy.* **2024**, *52*, 364-77. DOI
118. Biswas, R.; Dastider, S. G.; Ahmed, I.; Biswas, S.; Mondal, K.; Haldar, K. K. Bio-assisted synthesis of Au/Rh nanostructure electrocatalysts for hydrogen evolution and methanol oxidation reactions: composition matters. *Energy. Fuels.* **2023**, *37*, 13231-40. DOI
119. Guo, L.; Xu, W.; Sun, Z.; et al. Highly dispersed Rh prepared by the in-situ etching-growth strategy for energy-saving hydrogen evolution. *J. Taiwan. Inst. Chem. Eng.* **2022**, *132*, 104118. DOI
120. Hwang, G. S.; Shin, W.; Yim, G.; et al. Morphology-controlled silver-containing rhodium nanoparticles for the hydrogen evolution reaction. *J. Electrochem. Soc.* **2022**, *169*, 044517. DOI
121. Lu, R.; Sam, D. K.; Gong, S.; et al. Silk fibroin derived porous carbon aerogels confined hyperdispersed Rh nanoparticles to achieve electrocatalytic hydrogen evolution under high current density. *Diamond. Relat. Mater.* **2022**, *128*, 109292. DOI
122. Kim, J.; Kani, K.; Kim, J.; et al. Mesoporous Rh nanoparticles as efficient electrocatalysts for hydrogen evolution reaction. *J. Ind. Eng. Chem.* **2021**, *96*, 371-5. DOI
123. Mao, Q.; Jiao, S.; Ren, K.; et al. Transition metal and phosphorus co-doping induced lattice strain in mesoporous Rh-based nanospheres for pH-universal hydrogen evolution electrocatalysis. *Chem. Eng. J.* **2021**, *426*, 131227. DOI
124. Kumaravel, S.; Karthick, K.; Sankar, S. S.; Karmakar, A.; Kundu, S. Shape-selective rhodium nano-huddles on DNA for high efficiency hydrogen evolution reaction in acidic medium. *J. Mater. Chem. C* **2021**, *9*, 1709-20. DOI
125. Hu, M.; Chen, Q.; Ding, R.; Wu, J.; Wang, Y.; Zhang, Y.; Fan, G. Spatially localized fabrication of uniform Rh nanoclusters on nanosheet-assembled hierarchical carbon architectures as excellent electrocatalysts for boosting alkaline hydrogen evolution. *Int. J. Hydrogen. Energy.* **2020**, *45*, 8118-25. DOI
126. Akbayrak, M.; Önal, A. M. High durability and electrocatalytic activity toward hydrogen evolution reaction with ultralow rhodium loading on Titania. *J. Electrochem. Soc.* **2020**, *167*, 156501. DOI
127. Liu, M.; Hof, F.; Moro, M.; Valenti, G.; Paolucci, F.; Pénicaud, A. Carbon supported noble metal nanoparticles as efficient catalysts for electrochemical water splitting. *Nanoscale* **2020**, *12*, 20165-70. DOI PubMed
128. Su, L.; Zhao, Y.; Yang, F.; Wu, T.; Cheng, G.; Luo, W. Ultrafine phosphorus-doped rhodium for enhanced hydrogen electrocatalysis in alkaline electrolytes. *J. Mater. Chem. A* **2020**, *8*, 11923-7. DOI
129. Du, J.; Wang, X.; Li, C.; Liu, X.; Gu, L.; Liang, H. Hollow Rh nanoparticles with nanoporous shell as efficient electrocatalyst for hydrogen evolution reaction. *Electrochim. Acta.* **2018**, *282*, 853-9. DOI
130. Dang, Q.; Liao, F.; Sun, Y.; et al. Rhodium/silicon quantum dot/carbon quantum dot composites as highly efficient electrocatalysts for hydrogen evolution reaction with Pt-like performance. *Electrochim. Acta.* **2019**, *299*, 828-34. DOI
131. Huang, J.; Du, C.; Nie, J.; Zhou, H.; Zhang, X.; Chen, J. Encapsulated Rh nanoparticles in N-doped porous carbon polyhedrons derived from ZIF-8 for efficient HER and ORR electrocatalysis. *Electrochim. Acta.* **2019**, *326*, 134982. DOI
132. Wang, Q.; Xu, B.; Xu, C.; et al. Ultrasmall Rh nanoparticles decorated on carbon nanotubes with encapsulated Ni nanoparticles as excellent and pH-universal electrocatalysts for hydrogen evolution reaction. *Appl. Surf. Sci.* **2019**, *495*, 143569. DOI
133. Huang, X.; Wang, Y.; Zhu, Q.; Zhou, K.; Zhi, H.; Yang, J. High quality synthesis of Rh nanocubes and their application in hydrazine hydrate oxidation assisted water splitting. *Inorg. Chem. Commun.* **2021**, *134*, 109023. DOI
134. Shen, W.; Ge, L.; Sun, Y.; et al. Rhodium nanoparticles/F-doped graphene composites as multifunctional electrocatalyst superior to Pt/C for hydrogen evolution and formic acid oxidation reaction. *ACS. Appl. Mater. Interfaces.* **2018**, *10*, 33153-61. DOI PubMed
135. Zhang, N.; Shao, Q.; Pi, Y.; Guo, J.; Huang, X. Solvent-mediated shape tuning of well-defined rhodium nanocrystals for efficient electrochemical water splitting. *Chem. Mater.* **2017**, *29*, 5009-15. DOI
136. Qin, Q.; Jang, H.; Chen, L.; Nam, G.; Liu, X.; Cho, J. Low loading of RhP and RuP on N, P codoped carbon as two trifunctional electrocatalysts for the oxygen and hydrogen electrode reactions. *Adv. Energy. Mater.* **2018**, *8*, 1801478. DOI

-
137. Xin, H.; Sun, L.; Zhao, Y.; et al. Size-controllable Rh₂P nanoparticles on reduced graphene oxide toward highly hydrogen production. *Chem. Eng. J.* **2023**, *466*, 143277. DOI
138. Xin, H.; Sun, L.; Zhao, Y.; et al. Surpassing Pt hydrogen production from {200} facet-riched polyhedral Rh₂P nanoparticles by one-step synthesis. *Appl. Catal. B. Environ.* **2023**, *330*, 122645. DOI
139. Li, Z.; Feng, Y.; Liang, Y. L.; et al. Stable rhodium (IV) oxide for alkaline hydrogen evolution reaction. *Adv. Mater.* **2020**, *32*, e1908521. DOI PubMed
140. Yoon, D.; Seo, B.; Lee, J.; et al. Facet-controlled hollow Rh₂S₃ hexagonal nanoprisms as highly active and structurally robust catalysts toward hydrogen evolution reaction. *Energy. Environ. Sci.* **2016**, *9*, 850-6. DOI
141. Feng, Q.; He, H.; Sun, Y.; et al. Interfacial electronic interaction regulation of Rh₂P by combining N, P co-doped graphene for boosting hydrogen evolution reaction. *Ceram. Int.* **2024**, *50*, 10108-16. DOI
142. Wang, Z.; Li, X.; Zhang, H.; et al. Amorphous/crystalline RhFeP metallene for hydrazine-assisted water splitting. *Nanotechnology* **2024**, *35*, 225401. DOI PubMed
143. Wang, Y.; Fecher, G. H.; Subakti, S.; et al. Nano-scale new Heusler compounds NiRh₂Sb and CuRh₂Sb: synthesis, characterization, and application as electrocatalysts. *J. Mater. Chem. A.* **2023**, *11*, 2302-13. DOI
144. Deng, K.; Wang, W.; Lian, Z.; et al. A general synthesis of crystal phase controllable aerogels for efficient hydrogen evolution. *Small* **2023**, *19*, e2304181. DOI PubMed
145. Galdeano-Ruano, C.; Márquez, I.; Lopes, C. W.; et al. Ultra-low metal loading rhodium phosphide electrode for efficient alkaline hydrogen evolution reaction. *Int. J. Hydrogen. Energy.* **2024**, *51*, 1200-16. DOI
146. Yang, J.; Zhu, C.; Yang, C. J.; et al. Accelerating the hydrogen production via modifying the fermi surface. *Nano. Lett.* **2023**, *23*, 11368-75. DOI PubMed
147. Sun, H.; Li, L.; Humayun, M.; et al. Achieving highly efficient pH-universal hydrogen evolution by superhydrophilic amorphous/crystalline Rh(OH)₃/NiTe coaxial nanorod array electrode. *Appl. Catal. B. Environ.* **2022**, *305*, 121088. DOI
148. Bu, X.; Bu, Y.; Quan, Q.; et al. Superior electrocatalyst for all-pH hydrogen evolution reaction: heterogeneous Rh/N and S co-doped carbon yolk-shell nanospheres. *Adv. Funct. Mater.* **2022**, *32*, 2206006. DOI
149. Batugedara, T. N.; Brock, S. L. Role of noble- and base-metal speciation and surface segregation in Ni_xRh_xP nanocrystals on electrocatalytic water splitting reactions in Alkaline media. *Chem. Mater.* **2022**, *34*, 4414-27. DOI
150. Li, J.; Wang, X.; Yi, L.; et al. Plasma-assisted rhodium incorporation in nickel-iron sulfide nanosheets: enhanced catalytic activity and the Janus mechanism for overall water splitting. *Inorg. Chem. Front.* **2022**, *9*, 6237-47. DOI
151. Downes, C. A.; Van Allsburg, K. M.; Tacey, S. A.; et al. Controlled synthesis of transition metal phosphide nanoparticles to establish composition-dependent trends in electrocatalytic activity. *Chem. Mater.* **2022**, *34*, 6255-67. DOI
152. Pan, S.; Chang, C.; Luo, F.; Yang, Z. Efficient alkaline water splitting catalyzed by ultrafine rhodium telluride nanoparticles. *Chem. Commun.* **2022**, *58*, 13923-6. DOI PubMed
153. Yang, S.; Yang, X.; Wang, Q.; et al. Facet-selective hydrogen evolution on Rh₂P electrocatalysts in pH-universal media. *Chem. Eng. J.* **2022**, *449*, 137790. DOI
154. Zhang, Y.; Li, G.; Zhao, Z.; et al. Atomically isolated Rh sites within highly branched Rh₂Sb nanostructures enhance bifunctional hydrogen electrocatalysis. *Adv. Mater.* **2021**, *33*, e2105049. DOI PubMed
155. Mutinda, S. I.; Batugedara, T. N.; Brown, B.; Brock, S. L. Co_{2-x}Rh_xP nanoparticles for overall water splitting in basic media: activation by phase-segregation-assisted nanostructuring at the anode. *ChemCatChem* **2021**, *13*, 4111-9. DOI
156. Li, Y.; Guo, Y.; Yang, S.; et al. Mesoporous RhRu nanosponges with enhanced water dissociation toward efficient alkaline hydrogen evolution. *ACS. Appl. Mater. Interfaces.* **2021**, *13*, 5052-60. DOI PubMed
157. Mutinda, S. I.; Batugedara, T. N.; Brown, B.; Adeniran, O.; Liu, Z.; Brock, S. L. Rh₂P activity at a fraction of the cost? Co_{2-x}Rh_xP nanoparticles as electrocatalysts for the hydrogen evolution reaction in acidic media. *ACS. Appl. Energy. Mater.* **2021**, *4*, 946-55. DOI
158. Wu, X.; Wang, R.; Li, W.; Feng, B.; Hu, W. Rh₂P nanoparticles partially embedded in N/P-doped carbon scaffold at ultralow metal loading for high current density water electrolysis. *ACS. Appl. Nano. Mater.* **2021**, *4*, 3369-76. DOI
159. Xin, H.; Dai, Z.; Zhao, Y.; et al. Recording the Pt-beyond hydrogen production electrocatalysis by dirhodium phosphide with an overpotential of only 4.3 mV in alkaline electrolyte. *Appl. Catal. B. Environ.* **2021**, *297*, 120457. DOI
160. Yao, Y.; Wang, Z.; Zhang, R.; Zhang, L.; Feng, J.; Wang, A. Effective construction of 3D Rh/Rh₂P flake-like assembled heterostructures for efficient hydrogen evolution. *J. Alloys. Compd.* **2021**, *865*, 158864. DOI
161. Zhong, W.; Xiao, B.; Lin, Z.; et al. RhSe₂: a superior 3D electrocatalyst with multiple active facets for hydrogen evolution reaction in both acid and alkaline solutions. *Adv. Mater.* **2021**, *33*, e2007894. DOI PubMed

-
162. Pan, S.; Ma, S.; Chang, C.; Long, X.; Qu, K.; Yang, Z. Activation of rhodium selenides for boosted hydrogen evolution reaction via heterostructure construction. *Mater. Today. Phys.* **2021**, *18*, 100401. DOI
163. Luo, F.; Guo, L.; Xie, Y.; et al. Robust hydrogen evolution reaction activity catalyzed by ultrasmall Rh-Rh₂P nanoparticles. *J. Mater. Chem. A* **2020**, *8*, 12378-84. DOI
164. Liu, S.; Chen, Y.; Yu, L.; et al. A supramolecular-confinement pyrolysis route to ultrasmall rhodium phosphide nanoparticles as a robust electrocatalyst for hydrogen evolution in the entire pH range and seawater electrolysis. *J. Mater. Chem. A* **2020**, *8*, 25768-79. DOI
165. Singh, N.; Hiller, J.; Metiu, H.; McFarland, E. Investigation of the electrocatalytic activity of rhodium sulfide for hydrogen evolution and hydrogen oxidation. *Electrochim. Acta* **2014**, *145*, 224-30. DOI
166. Chi, J. Q.; Zeng, X. J.; Shang, X.; et al. Embedding RhP in N, P co-doped carbon nanoshells through synergetic phosphorization and pyrolysis for efficient hydrogen evolution. *Adv. Funct. Mater.* **2019**, *29*, 1901790. DOI
167. Yang, F.; Zhao, Y.; Du, Y.; et al. A monodisperse Rh₂P-based electrocatalyst for highly efficient and pH-universal hydrogen evolution reaction. *Adv. Energy Mater.* **2018**, *8*, 1703489. DOI
168. Kim, T.; Park, J.; Jin, H.; et al. A facet-controlled Rh₃Pb₂S₂ nanocage as an efficient and robust electrocatalyst toward the hydrogen evolution reaction. *Nanoscale* **2018**, *10*, 9845-50. DOI PubMed
169. Pu, Z.; Amiin, I. S.; He, D.; Wang, M.; Li, G.; Mu, S. Activating rhodium phosphide-based catalysts for the pH-universal hydrogen evolution reaction. *Nanoscale* **2018**, *10*, 12407-12. DOI PubMed
170. Duan, H.; Li, D.; Tang, Y.; et al. High-performance Rh₂P electrocatalyst for efficient water splitting. *J. Am. Chem. Soc.* **2017**, *139*, 5494-502. DOI
171. Jiang, B.; Sun, Y.; Liao, F.; et al. Rh-Ag-Si ternary composites: highly active hydrogen evolution electrocatalysts over Pt-Ag-Si. *J. Mater. Chem. A* **2017**, *5*, 1623-8. DOI
172. Jiang, B.; Yang, L.; Liao, F.; et al. A stepwise-designed Rh-Au-Si nanocomposite that surpasses Pt/C hydrogen evolution activity at high overpotentials. *Nano. Res.* **2017**, *10*, 1749-55. DOI
173. Jin, D.; Yu, A.; Lee, Y.; Kim, M. H.; Lee, C. Ni_xRh_{1-x} bimetallic alloy nanofibers as a pH-universal electrocatalyst for the hydrogen evolution reaction: the synthetic strategy and fascinating electroactivity. *J. Mater. Chem. A* **2020**, *8*, 8629-37. DOI
174. Nguyen, N. A.; Choi, H. S. Effect of Ni/Rh ratios on characteristics of Ni_xRh_y nanosponges towards high-performance hydrogen evolution reaction. *Data. Brief.* **2019**, *24*, 103941. DOI PubMed PMC
175. Li, H.; Sun, M.; Pan, Y.; et al. The self-complementary effect through strong orbital coupling in ultrathin high-entropy alloy nanowires boosting pH-universal multifunctional electrocatalysis. *Appl. Catal. B. Environ.* **2022**, *312*, 121431. DOI
176. Kang, Y.; Cretu, O.; Kikkawa, J.; et al. Mesoporous multimetallic nanospheres with exposed highly entropic alloy sites. *Nat. Commun.* **2023**, *14*, 4182. DOI PubMed PMC
177. Zhao, Y.; Bai, J.; Wu, X.; et al. Atomically ultrathin RhCo alloy nanosheet aggregates for efficient water electrolysis in broad pH range. *J. Mater. Chem. A* **2019**, *7*, 16437-46. DOI
178. Sarno, M.; Ponticorvo, E.; Scarpa, D. PtRh and PtRh/MoS₂ nano-electrocatalysts for methanol oxidation and hydrogen evolution reactions. *Chem. Eng. J.* **2019**, *377*, 120600. DOI
179. Li, Q.; Sun, C.; Fu, H.; et al. Enhanced alkaline hydrogen evolution reaction through lanthanide-modified rhodium intermetallic catalysts. *Small* **2024**, *20*, e2307052. DOI PubMed
180. Li, Q.; Zhang, B.; Sun, C.; et al. Enhanced alkaline hydrogen evolution reaction via electronic structure regulation: activating PtRh with rare earth Tm alloying. *Small* **2024**, *20*, e2400662. DOI PubMed
181. Nguyen, M. T.; Deng, L.; Yonezawa, T. Control of nanoparticles synthesized via vacuum sputter deposition onto liquids: a review. *Soft. Matter* **2021**, *18*, 19-47. DOI PubMed
182. Pelech, I.; Narkiewicz, U.; Kaczmarek, A.; Jędrzejewska, A.; Pelech, R. Removal of metal particles from carbon nanotubes using conventional and microwave methods. *Sep. Purif. Technol.* **2014**, *136*, 105-10. DOI
183. Hsieh, T. E.; Frisch, J.; Wilks, R. G.; Papp, C.; Bär, M. Impact of catalysis-relevant oxidation and annealing treatments on nanostructured GaRh alloys. *ACS. Appl. Mater. Interfaces* **2024**, *16*, 19858-65. DOI PubMed PMC
184. Zou, Y.; Jing, L.; Zhang, J.; et al. ALD-made noble metal high entropy alloy nanofilm with sub-surface amorphization for enhanced hydrogen evolution. *J. Mater. Chem. A* **2024**, *12*, 5668-78. DOI
185. Yan, S.; Yang, X.; Zhong, M.; et al. Better than Pt in all-pH media: a charge transfer modulating hydrogen adsorption in cobalt-rhodium alloy aerogel to boost hydrogen evolution. *Chem. Eng. J.* **2023**, *474*, 145777. DOI
186. Wei, M.; Sun, Y.; Zhang, J.; Ai, F.; Xi, S.; Wang, J. High-entropy alloy nanocrystal assembled by nanosheets with d-d electron interaction for hydrogen evolution reaction. *Energy. Environ. Sci.* **2023**, *16*, 4009-19. DOI
187. Jing, L.; Zou, Y.; Goei, R.; et al. Conformal noble metal high-entropy alloy nanofilms by atomic layer deposition for an enhanced hydrogen evolution reaction. *Langmuir* **2023**, *39*, 3142-50. DOI PubMed

-
188. Wei, M.; Sun, Y.; Ai, F.; Xi, S.; Zhang, J.; Wang, J. Stretchable high-entropy alloy nanoflowers enable enhanced alkaline hydrogen evolution catalysis. *Appl. Catal. B. Environ.* **2023**, *334*, 122814. DOI
189. Zhang, M.; Duan, Z.; Cui, L.; et al. A phosphorus modified mesoporous AuRh film as an efficient bifunctional electrocatalyst for urea-assisted energy-saving hydrogen production. *J. Mater. Chem. A.* **2022**, *10*, 3086-92. DOI
190. Tian, W.; Zhang, X.; Wang, Z.; et al. Amorphization activated RhPb nanoflowers for energy-saving hydrogen production by hydrazine-assisted water electrolysis. *Chem. Eng. J.* **2022**, *440*, 135848. DOI
191. He, Z.; Wang, H.; Yu, T.; et al. Trimetallic Au@RhCu core-shell nanodendrites as efficient bifunctional electrocatalysts toward hydrogen and oxygen evolution reactions. *ChemistrySelect* **2022**, *7*, e202103472. DOI
192. Jiang, X.; Dong, Z.; Zhang, Q.; et al. Decoupled hydrogen evolution from water/seawater splitting by integrating ethylene glycol oxidation on PtRh_{0.02}@Rh nanowires with Rh atom modification. *J. Mater. Chem. A.* **2022**, *10*, 20571-9. DOI
193. Nam, Y.; Jin, D.; Lee, C.; Lee, Y. Fe-Cu-Rh ternary alloy nanofibers as an outstanding pH-universal electrocatalyst for hydrogen evolution reaction: the catalytic roles of Fe depending on pH. *Appl. Surf. Sci.* **2023**, *611*, 155484. DOI
194. Jiang, A.; Chen, J.; Liu, S.; et al. Intermetallic rhodium alloy nanoparticles for electrocatalysis. *ACS. Appl. Nano. Mater.* **2021**, *4*, 13716-23. DOI
195. Chen, M. T.; Zhang, R. L.; Feng, J. J.; et al. A facile one-pot room-temperature growth of self-supported ultrathin rhodium-iridium nanosheets as high-efficiency electrocatalysts for hydrogen evolution reaction. *J. Colloid. Interface. Sci.* **2022**, *606*, 1707-14. DOI PubMed
196. Kani, K.; Lim, H.; Whitten, A. E.; et al. First electrochemical synthesis of mesoporous RhNi alloy films for an alkali-mediated hydrogen evolution reaction. *J. Mater. Chem. A.* **2021**, *9*, 2754-63. DOI
197. Zhang, M.; Xu, Y.; Wang, S.; et al. Polyethylenimine-modified bimetallic Au@Rh core-shell mesoporous nanospheres surpass Pt for pH-universal hydrogen evolution electrocatalysis. *J. Mater. Chem. A.* **2021**, *9*, 13080-6. DOI
198. Wang, Y.; Yu, B.; He, M.; et al. Eutectic-derived high-entropy nanoporous nanowires for efficient and stable water-to-hydrogen conversion. *Nano. Res.* **2021**, *15*, 4820-6. DOI
199. Xie, Y. X.; Cen, S. Y.; Ma, Y. T.; Chen, H. Y.; Wang, A. J.; Feng, J. J. Facile synthesis of platinum-rhodium alloy nanodendrites as an advanced electrocatalyst for ethylene glycol oxidation and hydrogen evolution reactions. *J. Colloid. Interface. Sci.* **2020**, *579*, 250-7. DOI PubMed
200. Han, Z.; Zhang, R.; Duan, J.; et al. Platinum-rhodium alloyed dendritic nanoassemblies: an all-pH efficient and stable electrocatalyst for hydrogen evolution reaction. *Int. J. Hydrogen. Energy.* **2020**, *45*, 6110-9. DOI
201. Karthick, K.; Mansoor Basha, A. B.; Sivakumaran, A.; Kundu, S. Enhancement of HER kinetics with RhNiFe for high-rate water electrolysis. *Catal. Sci. Technol.* **2020**, *10*, 3681-93. DOI
202. Jin, Y.; Chen, F.; Wang, J.; Guo, L.; Jin, T.; Liu, H. Lamellar platinum-rhodium aerogels with superior electrocatalytic performance for both hydrogen oxidation and evolution reaction in alkaline environment. *J. Power. Sources.* **2019**, *435*, 226798. DOI
203. Zhang, B.; Zheng, Y.; Xing, Z.; et al. Interfacial electron-engineered tungsten oxynitride interconnected rhodium layer for highly efficient all-pH-value hydrogen production. *J. Mater. Chem. A.* **2024**, *12*, 4484-91. DOI
204. Pan, S.; Li, C.; Xiong, T.; Xie, Y.; Luo, F.; Yang, Z. Hydrogen spillover in MoO_xRh hierarchical nanosheets boosts alkaline HER catalytic activity. *Appl. Catal. B. Environ.* **2024**, *341*, 123275. DOI
205. Wu, J.; Fan, J.; Zhao, X.; et al. Atomically dispersed MoO_x on rhodium metallene boosts electrocatalyzed alkaline hydrogen evolution. *Angew. Chem. Int. Ed.* **2022**, *61*, e202207512. DOI PubMed
206. Zhao, Y.; Yang, C.; Mao, G.; Su, J.; Cheng, G.; Luo, W. Ultrafine Rh nanoparticle decorated MoSe₂ nanoflowers for efficient alkaline hydrogen evolution reaction. *Inorg. Chem. Front.* **2018**, *5*, 2978-84. DOI
207. Sun, H.; Zhang, W.; Li, J.; et al. Rh-engineered ultrathin NiFe-LDH nanosheets enable highly-efficient overall water splitting and urea electrolysis. *Appl. Catal. B. Environ.* **2021**, *284*, 119740. DOI
208. Skibińska, K.; Kutyla, D.; Yang, X.; Krause, L.; Marzec, M. M.; Żabiński, P. Rhodium-decorated nanoconical nickel electrode synthesis and characterization as an electrochemical active cathodic material for hydrogen production. *Appl. Surf. Sci.* **2022**, *592*, 153326. DOI
209. Chen, M. T.; Duan, J. J.; Feng, J. J.; et al. Iron, rhodium-codoped Ni₂P nanosheets arrays supported on nickel foam as an efficient bifunctional electrocatalyst for overall water splitting. *J. Colloid. Interface. Sci.* **2022**, *605*, 888-96. DOI PubMed
210. Zheng, H.; Huang, X.; Gao, H.; et al. Decorating cobalt phosphide and rhodium on reduced graphene oxide for high-efficiency hydrogen evolution reaction. *J. Energy. Chem.* **2019**, *34*, 72-9. DOI
211. Gao, J.; Yu, W.; Liu, J.; et al. Regulation of hydrogen binding energy via oxygen vacancy enables an efficient trifunctional Rh-Rh₂O₃ electrocatalyst for fuel cells and water splitting. *J. Colloid. Interface. Sci.* **2024**, *664*, 766-78. DOI PubMed
212. Liu, X.; Chen, G.; Guo, Y.; et al. Fabric-like rhodium-nickel-tungsten oxide nanosheets for highly-efficient electrocatalytic H₂ generation in an alkaline electrolyte. *J. Colloid. Interface. Sci.* **2024**, *659*, 895-904. DOI PubMed

-
213. Higashi, T.; Seki, K.; Nandal, V.; et al. Understanding the activation mechanism of RhCrO_x cocatalysts for hydrogen evolution with nanoparticulate electrodes. *ACS Appl. Mater. Interfaces*. **2024**, *16*, 26325-39. DOI PubMed
214. Perumal, S.; Seo, J. Enhanced alkaline water splitting on cobalt phosphide sites by 4d metal (Rh)-doping method. *Int. J. Hydrogen. Energy*. **2023**, *48*, 22009-20. DOI
215. Nedić Vasiljević, B.; Jovanović, A. Z.; Mentus, S. V.; Skorodumova, N. V.; Pašti, I. A. Galvanic displacement of Co with Rh boosts hydrogen and oxygen evolution reactions in alkaline media. *J. Solid. State. Electrochem.* **2023**, *27*, 1877-87. DOI
216. Nguyen, N.; Chuluunbat, E.; Nguyen, T. A.; Choi, H. High electrocatalytic activity of Rh-WO₃ electrocatalyst for hydrogen evolution reaction under the acidic, alkaline, and alkaline-seawater electrolytes. *Int. J. Hydrogen. Energy*. **2023**, *48*, 32686-98. DOI
217. Bhuvanendran, N.; Park, C. W.; Su, H.; Lee, S. Y. Multifunctional Pt₂Rh-Co₃O₄ alloy nanoparticles with Pt-enriched surface and induced synergistic effect for improved performance in ORR, OER, and HER. *Environ. Res.* **2023**, *229*, 115950. DOI PubMed
218. Zhou, Y.; Hao, W.; Zhao, X.; et al. Electronegativity-induced charge balancing to boost stability and activity of amorphous electrocatalysts. *Adv. Mater.* **2022**, *34*, e2100537. DOI
219. Gao, Y.; Qi, L.; He, F.; Xue, Y.; Li, Y. Selectively growing a highly active interface of mixed Nb-Rh Oxide/2D carbon for electrocatalytic hydrogen production. *Adv. Sci.* **2022**, *9*, e2104706. DOI PubMed PMC
220. Wang, Y.; Luo, X.; Lu, W.; et al. Carbon supported bifunctional Rh-Ni(OH)₂/C nanocomposite catalysts with high electrocatalytic efficiency for alkaline hydrogen evolution reaction. *Int. J. Hydrogen. Energy*. **2022**, *47*, 13674-82. DOI
221. Jovanović, A. Z.; Bijelić, L.; Dobrota, A. S.; Skorodumova, N. V.; Mentus, S. V.; Pašti, I. A. Enhancement of hydrogen evolution reaction kinetics in alkaline media by fast galvanic displacement of nickel with rhodium - from smooth surfaces to electrodeposited nickel foams. *Electrochim. Acta*. **2022**, *414*, 140214. DOI
222. Wang, R.; Wang, X.; Cheng, M.; et al. Phosphatizing engineering of heterostructured Rh₂P/Rh nanoparticles on doped graphene for efficient hydrogen evolution in alkaline and acidic media. *Int. J. Hydrogen. Energy*. **2022**, *47*, 24669-79. DOI
223. Zhu, K.; Chen, J.; Wang, W.; et al. Etching-doping sedimentation equilibrium strategy: accelerating kinetics on hollow Rh-doped CoFe-layered double hydroxides for water splitting. *Adv. Funct. Mater.* **2020**, *30*, 2003556. DOI
224. Rodrigues, M. P. D. S.; Dourado, A. H. B.; Cutolo, L. D. O.; et al. Gold-rhodium nanoflowers for the plasmon-enhanced hydrogen evolution reaction under visible light. *ACS. Catal.* **2021**, *11*, 13543-55. DOI
225. Tran, P. K. L.; Tran, D. T.; Malhotra, D.; et al. Highly effective freshwater and seawater electrolysis enabled by atomic Rh-modulated Co-CoO lateral heterostructures. *Small* **2021**, *17*, e2103826. DOI PubMed
226. Wen, B. Y.; Chen, Q. Q.; Radjenovic, P. M.; Dong, J. C.; Tian, Z. Q.; Li, J. F. In situ surface-enhanced raman spectroscopy characterization of electrocatalysis with different nanostructures. *Annu. Rev. Phys. Chem.* **2021**, *72*, 331-51. DOI PubMed
227. Wen, J.; Tang, S.; Wu, X.; et al. Unraveling the mechanism of hydrogen evolution reactions in alkaline media: recent advances in in situ Raman spectroscopy. *Chem. Commun.* **2025**, *61*, 8778-89. DOI PubMed
228. Kim, J. H.; Jo, H. J.; Han, S. M.; Kim, Y. J.; Kim, S. Y. Recent advances in electrocatalysts for anion exchange membrane water electrolysis: design strategies and characterization approaches. *Energy. Mater.* **2025**, *5*, 500099. DOI PubMed
229. Zhang, X.; Guo, Y.; Wang, C. Multi-interface engineering of nickel-based electrocatalysts for alkaline hydrogen evolution reaction. *Energy. Mater.* **2024**, *4*, 400044. DOI PubMed
230. Aigbe, U. O.; Osibote, O. A. Green synthesis of metal oxide nanoparticles, and their various applications. *J. J. Hazard. Mater. Adv.* **2024**, *13*, 100401. DOI
231. Eweis, A. A.; El-Raheem, H. A.; Ahmad, M. S.; Hozzein, W. N.; Mahmoud, R. Green fabrication of nanomaterials using microorganisms as nano-factories. *J. Cluster. Sci.* **2024**, *35*, 2149-76. DOI
232. Kim, J.; Seo, J. H.; Lee, J. K.; Oh, M. H.; Jang, H. W. Challenges and strategies in catalysts design towards efficient and durable alkaline seawater electrolysis for green hydrogen production. *Energy. Mater.* **2025**, *5*, 500076. DOI PubMed
233. Wang, J.; Ma, J.; Du, H.; Ma, R.; Wang, J. Electrifying nitrate conversion: dual-metal-site catalysts as a game-changer for sustainable NH₃ production. *Nano. Res.* **2025**. DOI
234. Qiu, C.; Brinck, T.; Wang, J. Modeling the potential energy surface by force fields for heterogeneous catalysis: classification, applications, and challenges. *Chem. Sci.* **2025**, *16*, 21269-97. DOI PubMed PMC
235. Du, H.; Li, H.; Song, J.; et al. Reconstructing interfacial H-bond networks via surface lewis-base silicate species for durable seawater oxidation. *Adv. Funct. Mater.* **2025**, e25265. DOI

Disclaimer/Publisher's Note: All statements, opinions, and data contained in this publication are solely those of the individual author(s) and contributor(s) and do not necessarily reflect those of OAE and/or the editor(s). OAE and/or the editor(s) disclaim any responsibility for harm to persons or property resulting from the use of any ideas, methods, instructions, or products mentioned in the content.



© The Author(s) 2026. Open Access This article is licensed under a Creative Commons Attribution 4.0 International License (<https://creativecommons.org/licenses/by/4.0/>), which permits unrestricted use, sharing, adaptation, distribution and reproduction in any medium or format, for any purpose, even commercially, as long as you give appropriate credit to the original author(s) and the source, provide a link to the Creative Commons license, and indicate if changes were made.